THESIS

EXAMINING TRENDS IN SNOWMELT CONTRIBUTION TO STREAMFLOW IN THE SOUTHERN ROCKY MOUNTAINS OF COLORADO

Submitted by

Anna K. D. Pfohl

Department of Ecosystem Science and Sustainability

In partial fulfillment of the requirements

For the Degree of Master of Science

Colorado State University

Fort Collins, Colorado

Summer 2016

Master's Committee:

Advisor: Steven R. Fassnacht

John D. Stednick
Jeff Niemann

ABSTRACT

EXAMINING TRENDS IN SNOWMELT CONTRIBUTION TO STREAMFLOW IN THE SOUTHERN ROCKY MOUNTAINS OF COLORADO

Snowmelt contribution to streamflow in snow-dominated watersheds has largely been limited to using the Center of Volume method, which looks at the day at which a certain amount of flow has passed, typically 20%, 50%, and 80%, referred to as t_{Q20}, t_{Q50}, and t_{Q80}, respectively. We developed a new method to measure streamflow timing in the Southern Rocky Mountains of Colorado for 39 gauging stations from 1976 to 2015. We first manually extracted start and end days from the annual hydrograph of a small, medium, and large watershed to use as "truth." We then looked at the cumulative annual hydrograph and then found average spring and late fall baseflow. Using these average baseflows, we plotted the cumulative baseflow against the cumulative hydrograph and determined that the start and end of snowmelt contribution, t_{start} and t_{end}, occurred when the cumulative hydrograph departed from the cumulative baseflow by a given baseflow factor. Using NSE and RMSE values, we determined that 10x and 17.5 baseflow were able to best represent the manually extracted values. NSE values ranged from 0.59 to 0.6 and 0.53 to 0.69 for t_{start} and t_{end}, respectively; RMSE values ranged from 5.42 to 7.7 and 6.32 to 8.00, for t_{start} and t_{end}, respectively. In comparison, NSE values ranged from -4.73 to -25.35 and -5.87 to -13.25 for t_{Q20} and t_{Q80}, respectively; RMSE values ranged from 29.33 to 43.19 and 33.01 to 34.94 for t_{Q20} and t_{Q80}, respectively. This new automated method was able to better predict values of start and end than what has been commonly used in the literature.

We identified other variables related to snowmelt timing to streamflow, including the percent of flow and volume at the estimated t_{start} and t_{end}, as well as the total duration of contribution. We used the correlation coefficient to help explain the variance in the observed trends of the different snowmelt timing variables, using different physiographic characteristics (mean slope, mean elevation, mean solar radiation, latitude, and longitude) as well as trends in winter precipitation and summer NDVI. Most of these trends were not statistically significant, but mean slope was best able to explain the variance in trends for t_{end}, Q_{100}, Q_{end}, $Q_{duration}$, $\%Q_{tend}$, and t_{Q80} ($p < 0.05$).

ACKNOWLEDGEMENTS

I would like to thank my advisor, Dr. Steven Fassnacht, for his constant patience and guidance. I would also to thank my committee members Drs. John Stednick and Jeff Niemann for their contributions to this document and my graduate education. I would like to thank the Department of Ecosystem Science and Sustainability as well as the Vertically Integrated Projects Program at CSU for funding my education. Finally, I would also like to thank my parents for their endless support of my continued education.

TABLE OF CONTENTS

LIST OF TABLES

LIST OF FIGURES

Chapter 1: Introduction

Semi-arid and arid regions, like Colorado and much of the western United States, that receive little precipitation during the summer are particularly depend on snowmelt storage and reservoirs to supply water. In Colorado, snowfall comprises more than 60% of annual precipitation (Serreze et al., 1999). Snowmelt supplies a majority of water in Colorado, and the timing of snowmelt into streams is crucial for estimating water availability because snowmelt is an important characteristic for snow-dominated, high elevation watersheds (Schlaepfer et al., 2012). Snowmelt timing also plays an important role in other processes; for example, earlier snowmelt contribution has been linked with greater wildfire frequency (Westerling et al., 2006).

While the specifics of how climate change will affect Colorado streams is inconclusive (Clow, 2010), due in part to the complexity of snowmelt-dominated watersheds (Bales et al., 2006), research has suggested that there will be decrease in mountain snowpack (Stewart, 2009), which has implication for spring runoff and streamflow (Leung et al., 2005). Changes in snowmelt timing and its contribution to streamflow could require changes in reservoir storage capacity to accommodate an earlier melt (Barnett et al., 2005).

Prior to the 1960s, hydrologists characterized streamflow using two different methods. The first was using the momentary maximum, or the day of maximum discharge in a given year. The second was using the fraction of the total flow in a given month or a different length of time over the course of a year. These two methods, however, neglected a majority of the streamflow data in a given year (Court, 1962). The proposed alternative

was to use the half-flow data (now called the center of volume or COV as well as Center Timing or CT). This measure is simply the day at which 50% of the annual flow has passed and can be further divided into first and third quartile dates (Court, 1962).

The COV method has been adopted as a useful tool for streamflow timing metrics and been applied in numerous studies (Johnson, 1964; Satterlund and Eschner, 1965; Stewart et al., 2004; Stewart et al., 2005; Rauscher et al., 2008; Clow, 2010). The COV technique has been used as indicator of temporal trends in snowmelt generated streamflow (Stewart et al., 2005; Clow, 2010). However, the COV as an indicator of snowmelt timing may not be as useful or representative as originally thought. Based on model experiments as well as historical spring snowmelt data, COV may be more strongly influenced by total volume of streamflow than the timing of snowmelt (Whitfield, 2013). Change in timing of the COV may be indicative of changes in land use, precipitation timing, or baseflow (Johnson, 1964; Satterlund and Eschner, 1965; Whitfield, 2013), and therefore should be used with caution as an indicator of snowmelt timing.

Previous streamflow trend analyses

Trends in streamflow have been studied using various properties of the flow itself. Yue et al. (2002) used minimum and mean daily flows in a comparison of statistical methods for trend analysis and determined that the Mann-Kendall test in an appropriate metric in datasets without significant serial correlation. Yue and Pilon (2005) examined daily annual minimum flows in Canada to investigate the probability of regional low flow periods; while climatic and physiographic differences exist across different regions, they can be represented by the same distribution type. Ryberg et al. (2016) used peak streamflow annually as well as seasonally to identify trends across the Upper Midwest of

the United States and found that certain ecological regions are more sensitive to earlier snowmelt and spring peaks.

Streamflow has also been analyzed for climatic changes using the COV technique. The COV has been used in multiple studies that examine snowmelt contribution for mountainous regions and Colorado in particular. Across the western United States and Canada, there is an earlier onset of COV from 1948 to 2002 (Stewart et al., 2005). Most trends were statistically significant and predicted COV occurring anywhere from 5 to 20 days/decade later at stations in the Pacific Northwest. Few were statistically significant in the Southern Rocky Mountains, but observed changes in COV showed earlier onset of fewer than five days/decade (Stewart et al., 2005). Additionally, trends in the timing of COV were strongly correlated with changes in temperature from monthly gridded data but not precipitation (Stewart et al., 2005).

In another study conducted across the mountainous regions in the western United States, snowmelt-driven runoff (SDR) was estimated using the day at which 25%, 50%, and 75% of flow had passed for watersheds where at least half the annual runoff occurred from April to July (Rauscher et al., 2008); 25% and 75% of flow were used as proxies for the early and late season flows of SDR, respectively. Quartiles were used in addition to COV to attempt to eliminate sensitivities to false starts (Moore et al., 2007; Rauscher et al., 2008). Over their study period (1962-1987), 50% of SDR was occurring 2-10 days/decade earlier for regions in Colorado, but areas Idaho and California had smaller observed trends of 2-4 days/decade earlier (Rauscher et al., 2008). These trends were then applied to climate models with average global warming of 4˚C in the years 2071-2099, which predicted

earlier timing for 25%, 50% and 75% SDR by 14-40 days/decade for Colorado (Rauscher et al., 2008).

Discharge data and snow water equivalent (SWE) data from Snow Telemetry (SNOTEL) stations across Colorado were combined for water years 1978 to 2007 to estimate streamflow timing (Clow, 2010). This study used the day at which 20%, 50% (COV), and 80% of flow had passed, referred to as Q20, Q50, and Q80, respectively; Q20 and Q80 served as proxies for the start and end of snowmelt, respectively (Clow, 2010). Stations were grouped into thirteen different regions throughout Colorado and the Regional Kendall test was used to calculated trends. This metric showed an earlier onset for all percentages of annual flow. Trends were largest for Q20 and statistically significant at all regions, ranging from 4 to 12 days/decade earlier. For the COV, trends were statistically significant at all regions, ranging from 2 to 10 days/decade earlier. For Q80, trends were statistically significant at all but 2 of the 13 regions, ranging from 2 to 8 days/decade sooner (Clow, 2010). Results from the SNOTEL data indicate that high elevation watersheds are experience earlier snowmelt as well as earlier timing on the day at which 50% of snowpack has melted, and snowmelt onset is occurring as much as 8 days earlier (Clow, 2010).

Snowmelt in particular is occurring more quickly, especially in areas where winter precipitation has already decreased (Barnett et al., 2005). Daily SNOTEL data from 1984 to 2009 were used to examine trends in snowpack for several regions in the western United States. The length of snow-covered season is decreasing across study area. For Colorado in particular, they observed faster rates of snowmelt as well as decreased maximum SWE (Harpold et al., 2012).

Questions and Objectives

While changes in streamflow in high elevation, snowmelt-dominated watersheds have been studied before (Stewart et al., 2004; Stewart et al., 2005; Fassnacht, 2006; Rauscher et al., 2008; Clow, 2010; Fritze et al., 2011), the timing of snowmelt contribution to streamflow has largely been limited to finding a specific day (typically the COV) or days at which a given percentage of flow has passed. Large precipitation events influence the days at which COV and percentages of total annual flow occur and therefore may give results that are not representative of snowmelt timing (Whitfield, 2013). Additionally, COV can be more strongly influenced by inter-annual variability in streamflow volume than snowmelt timing (Whitfield, 2013). These examples demonstrate that COV should be employed with greater caution and that there is a need for a new method for streamflow timing that is more representative of snowmelt timing. Streamflow timing and related trends are important to study because of recent warming and subsequent ramifications in order to gain a better understanding of when snowmelt will occur for future use (Barnett et al., 2005).

How do the results from a new, automated methodology of estimating snowmelt timing and streamflow compare to results from using the COV technique? In this research, we developed a new methodology to automate and approximate when snowmelt was contributing to streamflow. By manually extracting the start and end of snowmelt contribution from the annual hydrograph at three different-sized basins (used as "truth"), we compared the derived values of start and end of snowmelt contribution from the new method and the COV technique and evaluate which method is better at predicting these dates. Additionally, we identified trends in snowmelt timing variables to compare the

results from the two methods. Finally, we explored the causes of the observed variance with different physiographic characteristics of the watershed and with observed trends in precipitation and land use.

Chapter 2: Methods

Data

We examined trends in streamflow timing for 40 years (1976 through 2015) in headwater streams across the Southern Rocky Mountains of Colorado (Figure 1). Streamflow data were collected from 39 gauging stations monitored by the United States Geological Survey (USGS) and available through the National Water Information System <http://waterdata.usgs.gov/co/nwis/rt>. Stations were selected based on having at least 30 years of record; for a specific water year to be included in analysis, it could not be missing more than 30 days of data. Basins were no larger than 1000 km^2 and ranged in size from 4 km^2 to 878 km^2, and station elevations were at least 2000 masl (Table 1).

Manual Extraction

In order to compare the automated values with those from the percent of annual flow (t_{Q20}, t_{Q50}, and t_{Q80}), we manually extracted the start and end of snowmelt contribution to streamflow for three watersheds with small, medium, and large areas: Michigan River, Black Gore Creek, and Crystal River. Because the hydrographs are baseflow-dominated until snowmelt begins, we were able to determine the start of contribution by looking at the annual hydrographs over the 40-year study period. To determine the start of snowmelt contribution, we looked for when the first initial increase in streamflow occurred; end of snowmelt was when the hydrograph started to return to baseflow (Figure 2). For each station, we conducted the manual extraction three times to ensure consistency in choosing values and eliminate any potential bias.

We then used the Root-Mean-Square Error (RMSE) (Equation 1) and the Nash-Sutcliffe Efficiency (NSE) (Equation 2) to assess how well t_{start}, t_{end}, t_{Q20}, and t_{Q80} predicted the start of snowmelt contribution and return to baseflow.

$$RMSE = \sqrt{\frac{1}{n}\sum_{i=1}^{n}(O_i - M_i)^2} \qquad \text{(Equation 1)}$$

$$NSE = 1 - \frac{\sum_{i=1}^{n}(O_i - M_i)^2}{\sum_{i=1}^{n}(O_i - \bar{O})^2} \qquad \text{(Equation 2)}$$

Existing Methodology

We calculated the day of the Water Year at which 20%, 50%, and 80% of flow had passed to compare timing with an automated method. Clow (2010) used 20% and 80% of flow as proxies for the start and end of snowmelt contribution, respectively, and 50% of flow, the COV, has been widely applied in streamflow timing (Stewart et al., 2004; Rauscher et al., 2008; Clow, 2010). We first found the total annual flow (Q_{100}) at each station-year and then found the days that corresponded with 20%, 50%, and 80% of flow, t_{Q20}, t_{Q50}, and t_{Q80}, respectively.

Automatic Timing Estimation

We decided to use the calendar year instead of water year because of precipitation events that occur in October (Fassnacht, 2006) (Figure 3). We used the cumulative annual hydrograph to estimate when snowmelt was contributing to streamflow. Because of the high elevation of these watersheds, streams are baseflow-dominated during the winter. During the spring and summer, the hydrograph shifts to snowmelt-dominated; this shift is

apparent on the cumulative hydrograph by changes in slope (Figure 4). At each station-year, we first found the average baseflow at the beginning of the year (January through mid-March) and at the end of the year (September through December). We then plotted the average cumulative spring and fall baseflow against the cumulative annual streamflow to identify when the cumulative streamflow departed from the average baseflow. We determined the start of snowmelt contribution (t_{start}) was when the difference between cumulative streamflow and cumulative baseflow was greater than 10 times the average baseflow and return to baseflow (t_{end}) was when the difference was 17.5 times the average baseflow (Figure 5; Figure 6). We conducted a sensitivity analysis to determine which baseflow factor best predicted streamflow timing and maximized NSE and minimized RMSE. We calculated the duration of snowmelt contribution to streamflow by subtracting the day of t_{start} from t_{end}. We also looked at the volume as well as percent of annual flow that had passed at t_{start} and t_{end}.

In order to compare the results of this developed methodology with the COV technique, we looked at the specific date at which our timing variables occurred instead of using Julian Day or day of water year.

Physiographic Characteristics of Watersheds

Other studies that have examined trends in snowmelt contribution to streamflow primarily relied on climatic indices to explain their observations (Stewart et al., 2004; Clow, 2010; Harpold et al., 2012). We chose to include several physical attributes to evaluate characteristics that could influence the trends in the hydrograph snowmelt characteristics. These included basin elevation, slope, and incoming winter solar radiation from October to March (Meromy et al., 2013). First, the 30-m digital elevation model was

acquired from the National Elevation Database (<http://nationalmap.gov/elevation.html>). Second, each watershed was delineated based on the location of the gauging station using the suite of hydrology tools in ArcGIS (<http://www.esri.com>). Third, the slope and aspect were computed using the ArcGIS surface tools. Finally, the mean elevation and mean slope were computed using the ArcGIS zonal statistics tools. We computed incoming solar radiation on the 15th of each month in October, November, December, January, February, and March within each watershed using the Area Solar Radiation tool, which calculates the insolation at the input landscape (Meromy et al., 2013). Finally, we found the mean of these six months to determine total winter incoming solar radiation.

To evaluate possible changes in snowmelt contribution to streamflow due to climate, monthly spatial precipitation data were acquired from the PRISM dataset (<http://www.prism.oregonstate.edu/>) for the winter months (October through March). These were available starting in 1982 at a resolution of 4 km. Because of the coarse resolution of the dataset, pixel size was greater than the size of 4 of the 39 basins. We used the resample tool by the nearest neighbor to change the resolution to that of the 30-m digital elevation model in order to include all basins in the precipitation analysis. For a given water year, the total precipitation that fell in each basin was computed using the ArcGIS zonal statistics tool.

In order to address any changes within the watershed from land use, beetle-kill, wildfires, or vegetation, we collected Normalized Difference Vegetation Index (NDVI) data from the USGS (<http://earthexplorer.usgs.gov/>). However, these data were available starting in July 1989 but are still an accurate representation of changes because major fires and beetle-kill areas didn't occur in the Southern Rocky Mountains until the late 1990s and

early 2000s (Wehner, 2016). We collected NDVI layers for July from 1989 to 2015 and found the NDVI for each watershed using the Zonal Statistics tool within ArcGIS.

Statistical Analyses

At each station, we conducted three different statistical analyses: the Mann-Kendall Test, Thiel-Sen's Slope, and Pearson's Correlation Coefficient. The Mann-Kendall Test is used to calculate the statistical significance of the trends in the snowmelt timing variables (t_{start}, t_{end}, Q_{100}, Q_{start}, Q_{end}, $Q_{duration}$,$\%Q_{tstart}$, $\%Q_{tend}$, t_{Q20}, t_{Q50}, and t_{Q80}), and the Thiel-Sen's Slope to quantify the rate of change (Salmi et al., 2002). For example, each station was given a value along with the level of statistical significance ($p < 0.05$) as well as the change in days per decade of the timing variable.

The correlation coefficient is used to determine relationship between two different sets of variables. We used the correlation coefficient to examine the relationships between the trends in the annual calculated variables (t_{start}, t_{end}, Q_{100}, Q_{start}, Q_{end}, $Q_{duration}$,$\%Q_{tstart}$, $\%Q_{tend}$, t_{Q20}, t_{Q50}, and t_{Q80}) and winter precipitation, NDVI, winter incoming solar radiation, mean elevation, and mean slope.

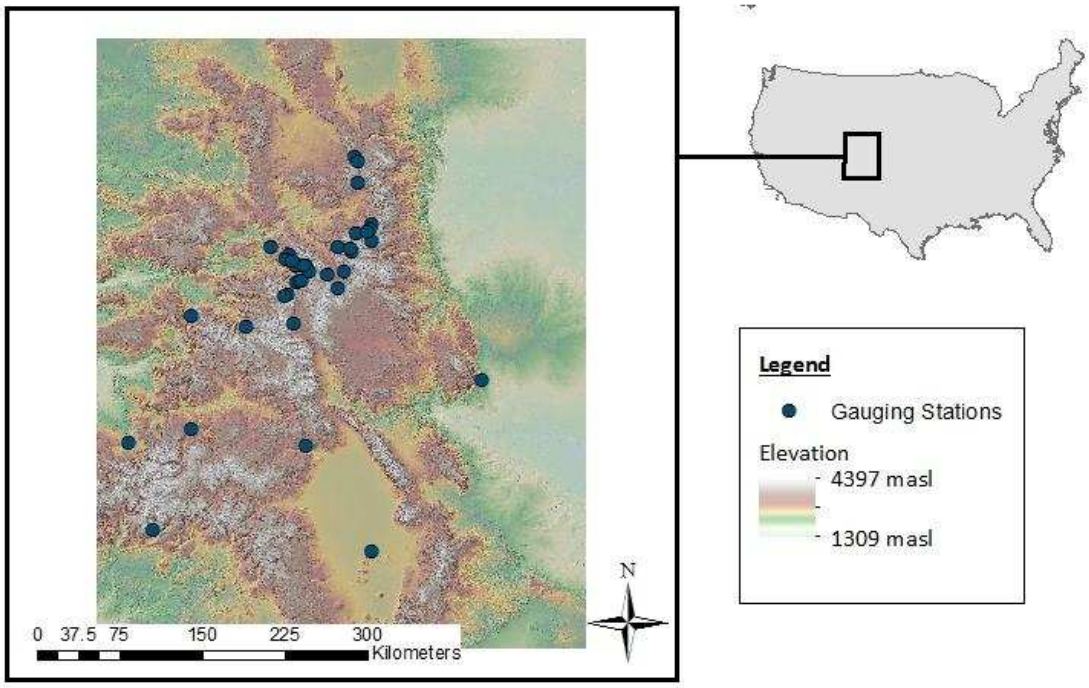

Figure 1. Distribution of USGS gauging stations in the Southern Rocky Mountains.

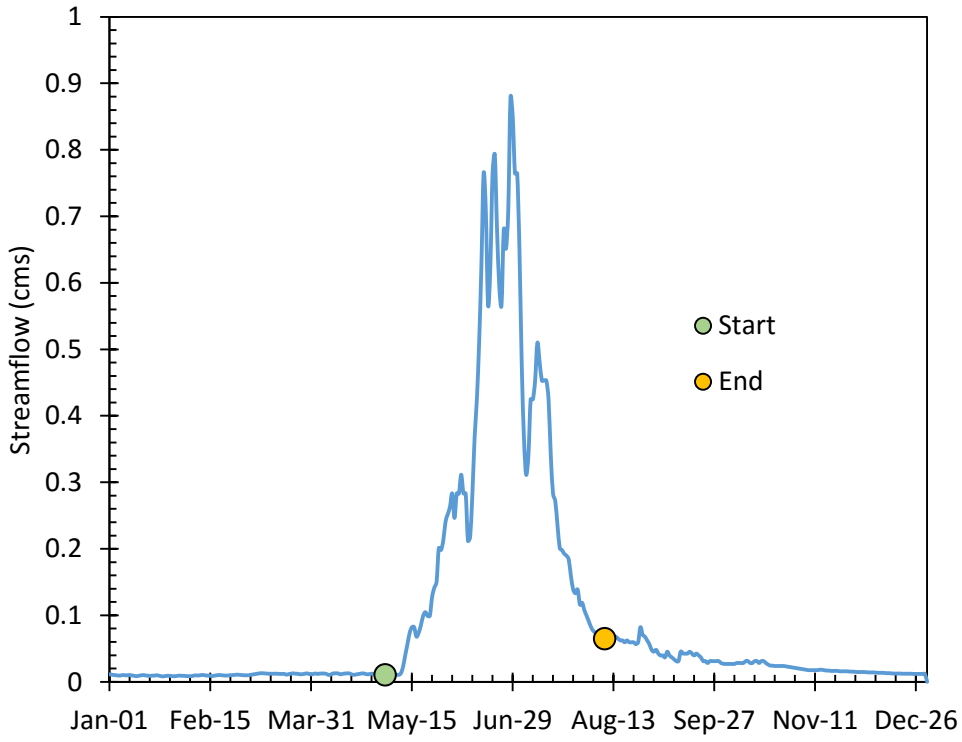

Figure 2. Example of the manually extracted start and end dates from Michigan River in 1993.

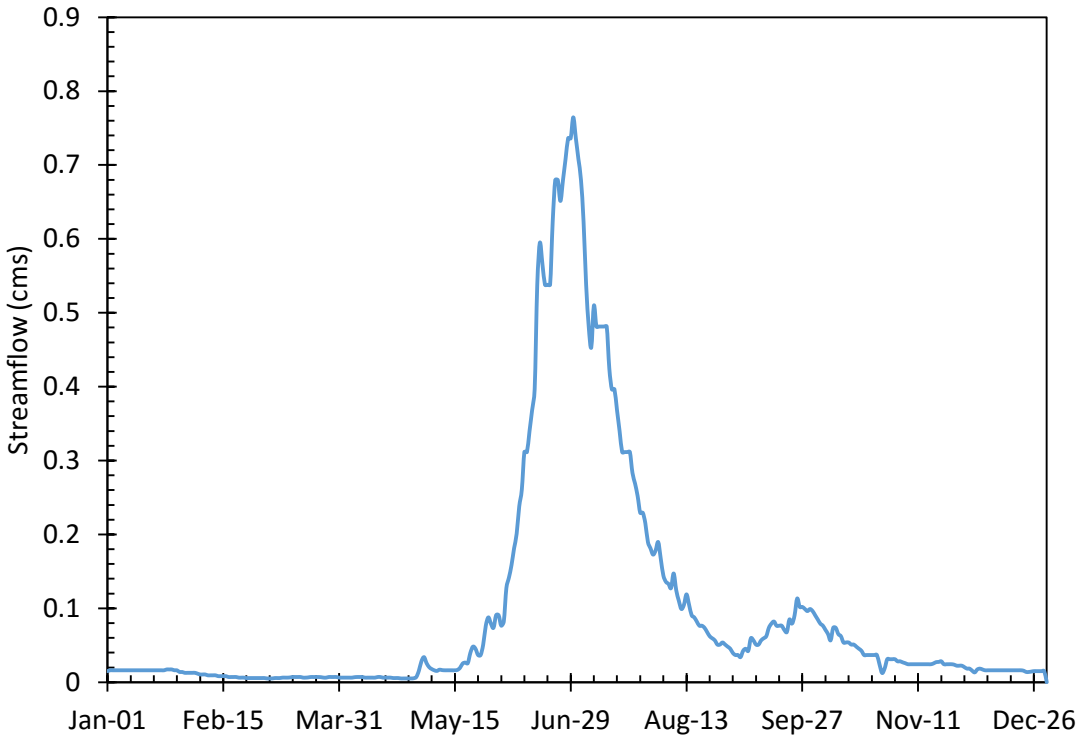

Figure 3. Example of late summer, early fall precipitation and why we chose to use calendar year instead of water year in our analysis.

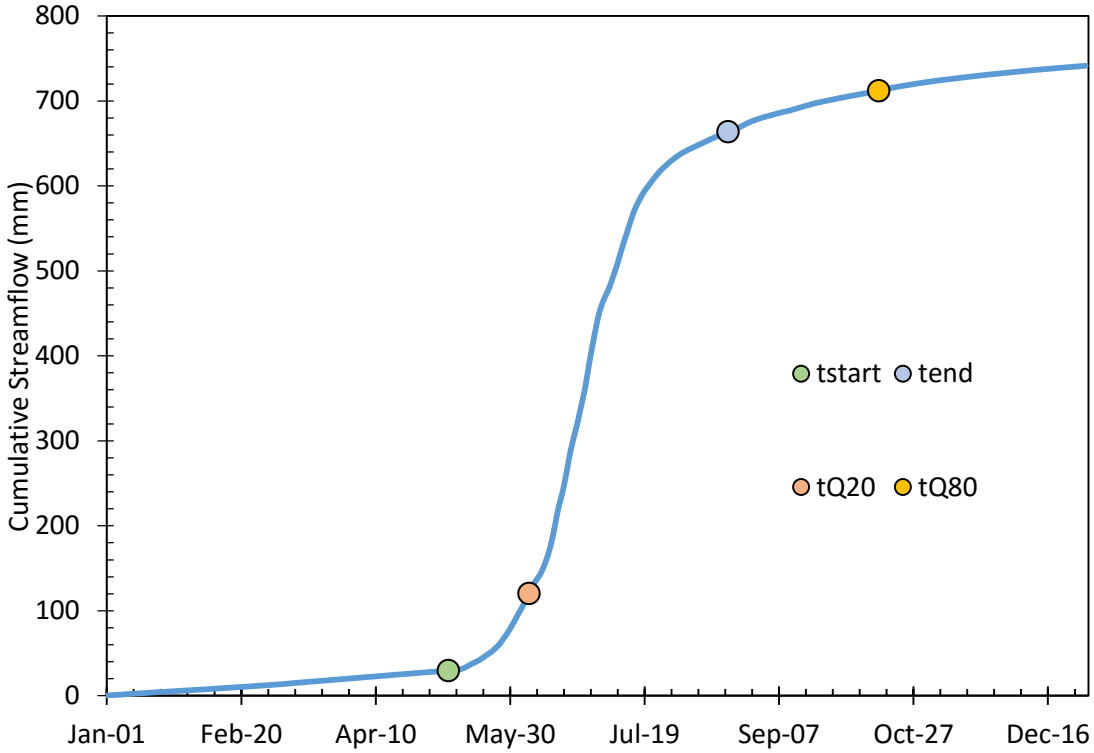

Figure 4. Sample annual cumulative hydrograph from Michigan River in 1993.

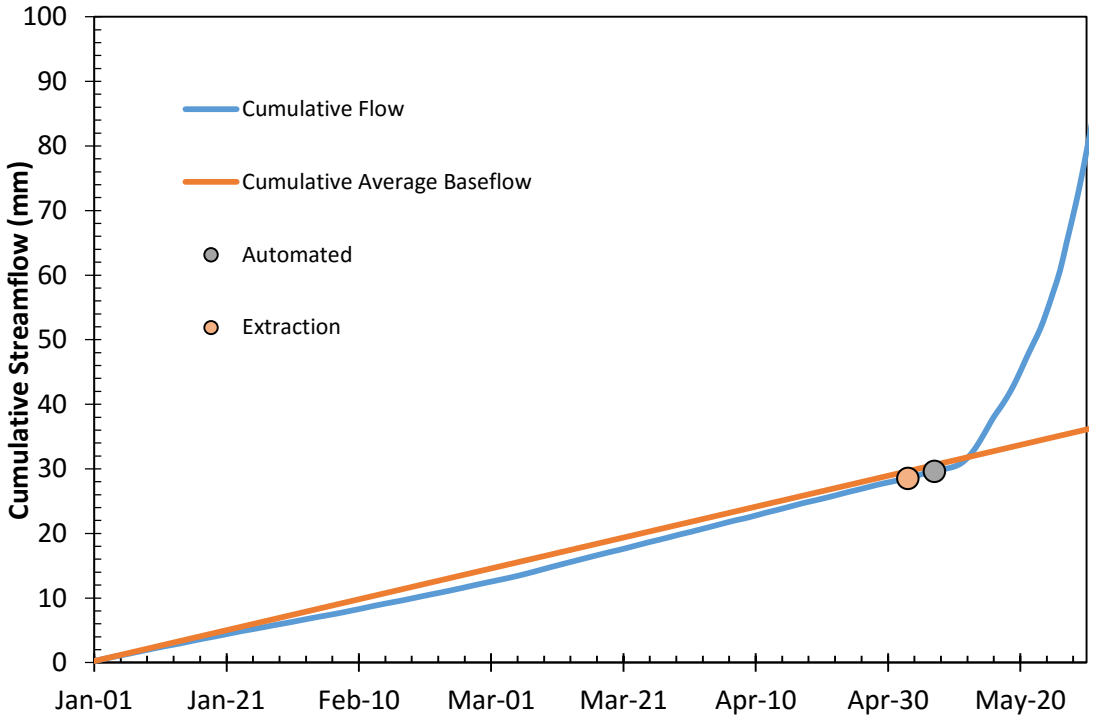

Figure 5. Example of the automated and manually extracted start days from Michigan River in 1993.

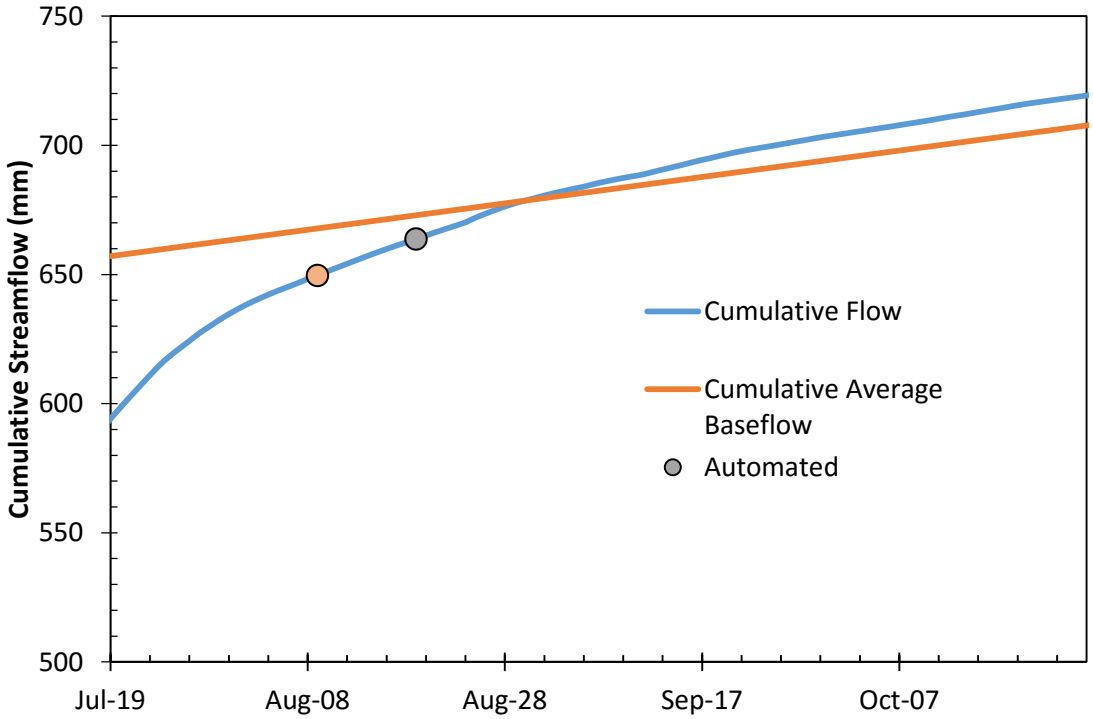

Figure 6. Example of the automated and manually extracted end days from Michigan River in 1993.

Table 1. USGS gauging stations used in analysis with station and basin information.

HUC Code	Station Name	Latitude	Longitude	Elevation (m)	Area (km^2)
9066100	Bighorn Creek	39.63999	-106.293	2629	12
9066000	Black Gore Creek	39.59637	-106.265	2789	32
9046600	Blue River	39.45582	-106.032	2749	319
9034900	Bobtail Creek	39.76026	-105.906	3179	15
9066200	Booth Creek	39.64832	-106.323	2537	16
9032100	Cabin Creek	39.98582	-105.745	2914	13
9010500	Colorado River	40.32582	-105.857	2667	165
8245000	Conejos River	37.30029	-105.747	3007	104
9081600	Crystal River	39.23264	-107.228	2105	433
9035800	Darling Creek	39.79719	-106.026	2725	23
9058610	Dickson Creek	39.70411	-106.457	2818	9
9063000	Eagle River	39.50832	-106.367	2638	182
9058800	East Meadow Creek	39.73165	-106.427	2882	9
9022000	Fraser River	39.84582	-105.752	2902	27
9058700	Freeman Creek	39.69832	-106.446	2845	8
9065500	Gore Creek	39.62582	-106.278	2621	38
7083000	Halfmoon Creek	39.17221	-106.389	2996	61
9064000	Homestake Creek	39.40554	-106.433	2804	92
6746095	Joe Wright Creek	40.53998	-105.883	3045	8
9047700	Keystone Gulch	39.59443	-105.973	2850	24
9124500	Lake Fork	38.29888	-107.23	2386	878
6614800	Michigan River	40.49609	-105.865	3167	4
9066300	Middle Creek	39.64582	-106.382	2499	15
9063900	Missouri Creek	39.39026	-106.47	3042	17
9059500	Piney River	39.79572	-106.574	2217	219
9066150	Pitkin Creek	39.6436	-106.303	2598	14
9032000	Ranch Creek	39.94999	-105.766	2640	52
9066400	Red Sandstone Creek	39.68276	-106.401	2808	19
9073300	Roaring Fork River	39.1411	-106.774	2475	196
7105945	Rock Creek	38.70749	-104.847	2000	18
9035900	S Fork of Williams	39.80054	-106.026	2728	71
9026500	St. Louis Creek	39.90999	-105.878	2737	85
9050100	Tenmile Creek	39.57526	-106.111	2774	239
9063400	Turkey Creek	39.5226	-106.337	2718	61
9146200	Uncompahgre River	38.18388	-107.746	2096	386
9352900	Vallecito Creek	37.4775	-107.544	2410	188
9025000	Vasquez Creek	39.92026	-105.785	2673	72
9063200	Wearyman Creek	39.52221	-106.324	2829	25
9035500	Williams Fork	39.77888	-105.928	2987	42

Table 2. NSE and RMSE values for t_{Q20} and the baseflow factors for t_{start}.

	NSE			RMSE		
Baseflow Factor	Black Gore	Michigan River	Crystal River	Black Gore	Michigan River	Crystal River
5	-1.17	-0.40	0.13	13.46	14.47	8.00
7.5	0.04	0.26	0.49	8.96	10.56	6.14
10	0.59	0.60	0.60	5.85	7.79	5.42
12.5	0.55	0.61	0.56	6.11	7.64	5.72
15	0.41	0.66	0.56	6.11	7.64	0.00
20	-0.20	0.53	0.32	10.01	8.43	0.00
25	-0.90	0.20	-0.06	12.59	10.96	8.87
t_{Q20}	-13.75	-4.73	-25.35	35.07	29.33	43.19

Table 3. NSE and RMSE values for t_{Q80} and the baseflow factors for t_{end}.

	NSE			RMSE		
Baseflow Factor	Black Gore	Michigan River	Crystal	Black Gore	Michigan River	Crystal
10	0.23	0.03	0.39	9.90	10.12	10.46
15	0.66	0.40	0.63	6.57	7.99	8.15
17.5	0.69	0.53	0.64	6.32	7.04	8.00
20	0.65	0.51	0.61	6.77	7.20	8.32
22.5	0.56	0.46	0.54	7.48	7.58	9.05
25	0.43	0.38	0.44	8.54	8.12	9.96
30	0.12	0.16	0.21	10.58	9.44	11.85
t_{q80}	-13.25	-9.31	-5.87	42.54	33.01	34.94

Chapter 3: Results

In order to determine the baseflow factor used to identify t_{start} and t_{end}, we compared NSE and RMSE values from several different multiplication factors and ultimately chose the factors that were best across the three different sample watersheds (Figure 7; Figure 8). The automatic timing estimation method resulted in higher NSE and lower RMSE values than using tq20 or tq80 when trying to predict the "truth" taken from the manually extracted values for snowmelt timing (Table 2; Table 3).

Trends in Snowmelt Timing Variables

At the start of snowmelt contribution, t_{start} trends ranged from occurring 7.3 days/decade later to 4.2 days/decade earlier, with statistical significance ($p < 0.05$) at 15 stations; t_{Q20} trends had a greater range, from 8.8 days/decade later to 12.3 days/decade earlier, with statistical significance at 2 stations (Figure 9). At the end of snowmelt contribution, t_{end} trends ranged from occurring 8.7 days/decade later to 6.5 days/decade earlier, with statistical significance at 9 stations; t_{Q80} trends had a smaller range, from 4 days/decade later to 5 days/decade earlier, with statistical significance at 4 stations (Figure 10). For the total duration of snowmelt contribution to streamflow, $tQ_{duration}$ trends ranged from 2.1 to 37.1 days/decade earlier, with statistical significance at 37 stations (Figure 11); $t_{duration}$ trends had a smaller range, from 9.1 days/decade later to 6.6 days/decade earlier, with statistical significance at 2 stations (Figure 12).

For the other timing variables, Q_{start} ranged from 11.6 mm/decade less water to 19.2 mm/decade more, with statistical significance at 10 stations (Figure 13), where Q_{end} had a larger range, from 95.5 mm/decade less water to 73.5 mm/decade more, with statistical

significance at 2 stations (Figure 14). Total annual volume (Q_{100}) ranged from having 80.7 mm/decade less to 185 mm/decade more water, with statistical significance at 3 stations (Figure 15). The percentage of annual flow that occurred at t_{start}, $\%Q_{tstart}$, ranged from 0.8 %/decade less to 2.5 %/decade more, with statistical significance at 4 stations; $\%Q_{tend}$ ranged from 2.8 %/decade less to 4.5 %/decade more, with statistical significance at 3 stations (Figure 16).

Physiographic Characteristics

Trends in NDVI indicated that there were few disturbances within the watersheds with changes in NDVI ranging from 1%/decade to 7%/decade, with statistical significance at 4 stations (Figure 17). Winter precipitation trends varied from 53.8 mm/decade less to 2.3 mm/decade more, with statistical significance at 7 stations (Figure 18).

Mean elevation ranged from 2494 to 3644 masl, and 35 of the 39 stations had mean elevations greater than 3000 masl. Mean slope ranged from 9˚ to 26˚. Incoming winter solar radiation ranged from 1407 to 1760 Watt-Hours/m^2 (Table 4).

Correlation Coefficient

There was positive correlation between radiation and t_{start}, Q_{start}, , Q_{end}, $Q_{duration}$, $\%Q_{tstart}$, and $\%Q_{tend}$, and negative correlation between radiation and t_{end}, $t_{duration}$, Q_{100}, t_{Q20}, t_{Q50}, t_{Q80}, and $t_{Qduration}$, but none of these relationships were statistically significant. There was positive correlation between elevation t_{start}, Q_{100}, Q_{start}, $\%Q_{tstart}$, and $\%Q_{tend}$, and negative correlation between elvation and t_{end}, $t_{duration}$, Q_{end}, $Q_{duration}$, t_{Q20}, t_{Q50}, t_{Q80}, and $t_{Qduration}$; only t_{Q80} had a statistically significant relationship ($p < 0.05$). There was a negative correlation between slope and all snowmelt timing variables, and these relationships were statistically significant for at t_{end}, Q_{100}, Q_{end}, $Q_{duration}$, and t_{Q20} $p < 0.05$, and t_{Q50} at $p < 0.10$.

There was a positive correlation between latitude and t_{start}, t_{end}, $t_{duration}$, Q_{100}, Q_{start}, Q_{end}, $Q_{duration}$, $\%Q_{tstart}$, $\%Q_{tend}$, t_{Q20}, and t_{Q50}, and negative correlation between latitude t_{Q80} and $t_{Qduration}$. These relationships were statistically significant for Q_{100}, Q_{end}, $\%Q_{tend}$, and t_{Q80}. There was a positive correlation between longitude and t_{start}, Q_{start}, $\%Q_{tstart}$, and $t_{Qduration}$, and a negative correlation between longitude and t_{end}, $t_{duration}$, Q_{100}, Q_{end}, $Q_{duration}$, $\%Q_{tend}$, t_{Q20}, t_{Q50}, and t_{Q80}. These relationships were statistically significant for t_{Q50} ($p < 0.05$) and t_{end}, $t_{duration}$, and t_{Q80} ($p < 0.10$) (Table 5).

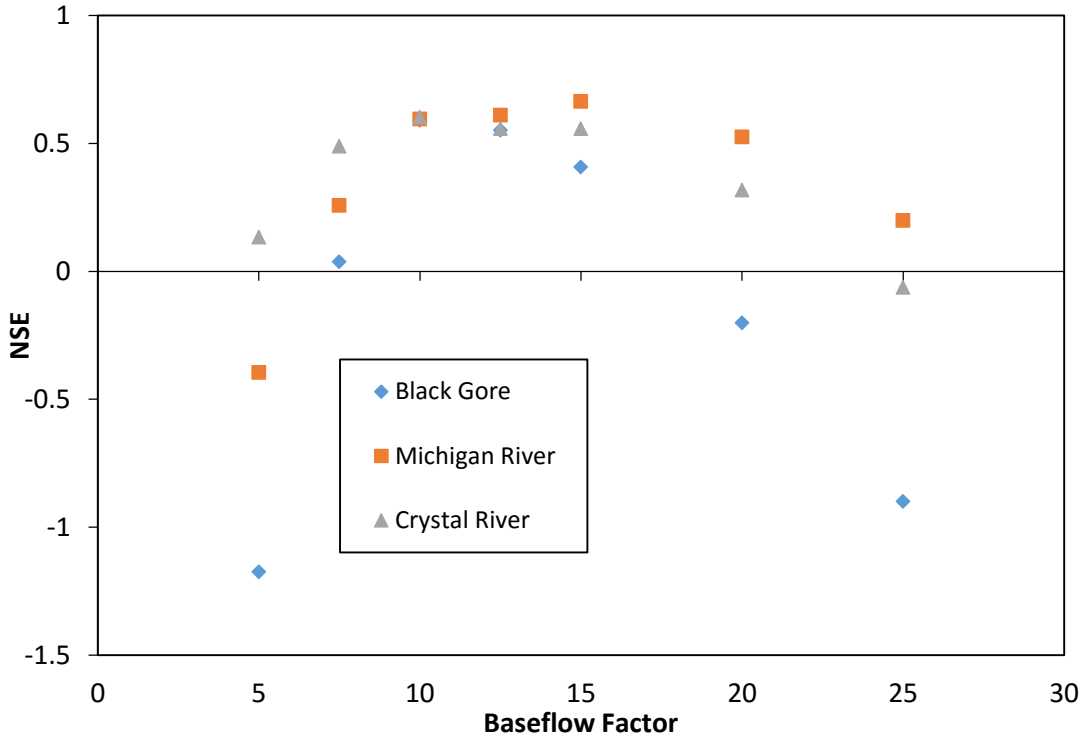

Figure 7. Comparison of NSE values for the baseflow factor for the start of snowmelt contribution.

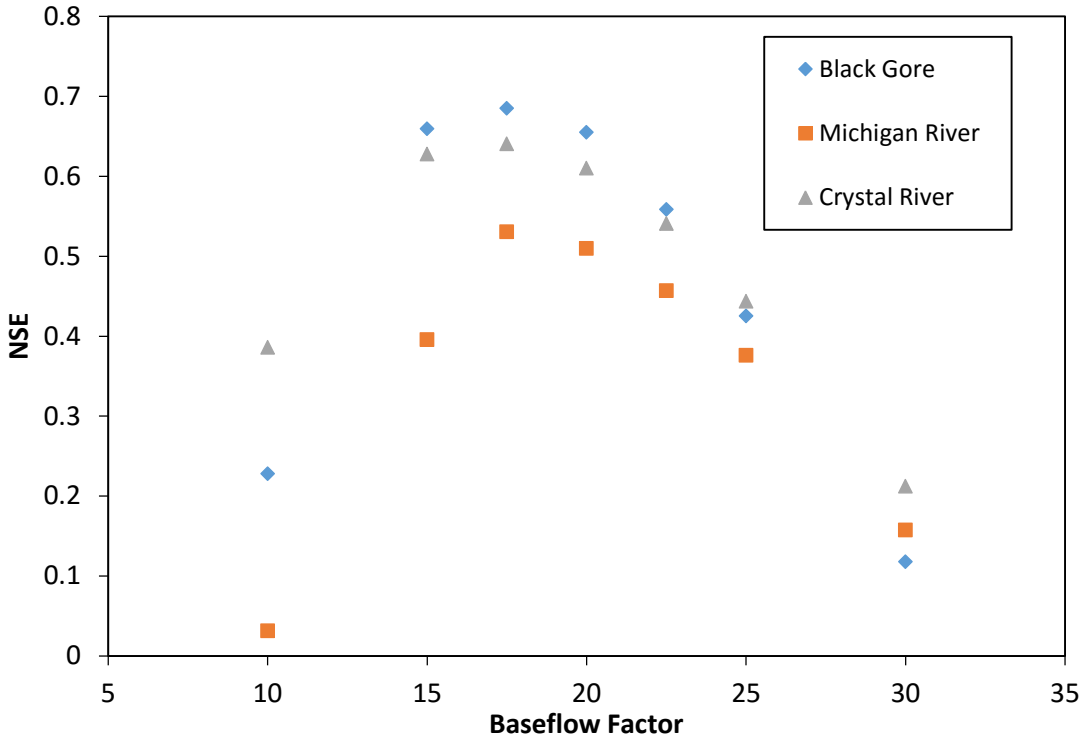

Figure 8. Comparison of NSE values for the baseflow factor for the end of snowmelt contribution.

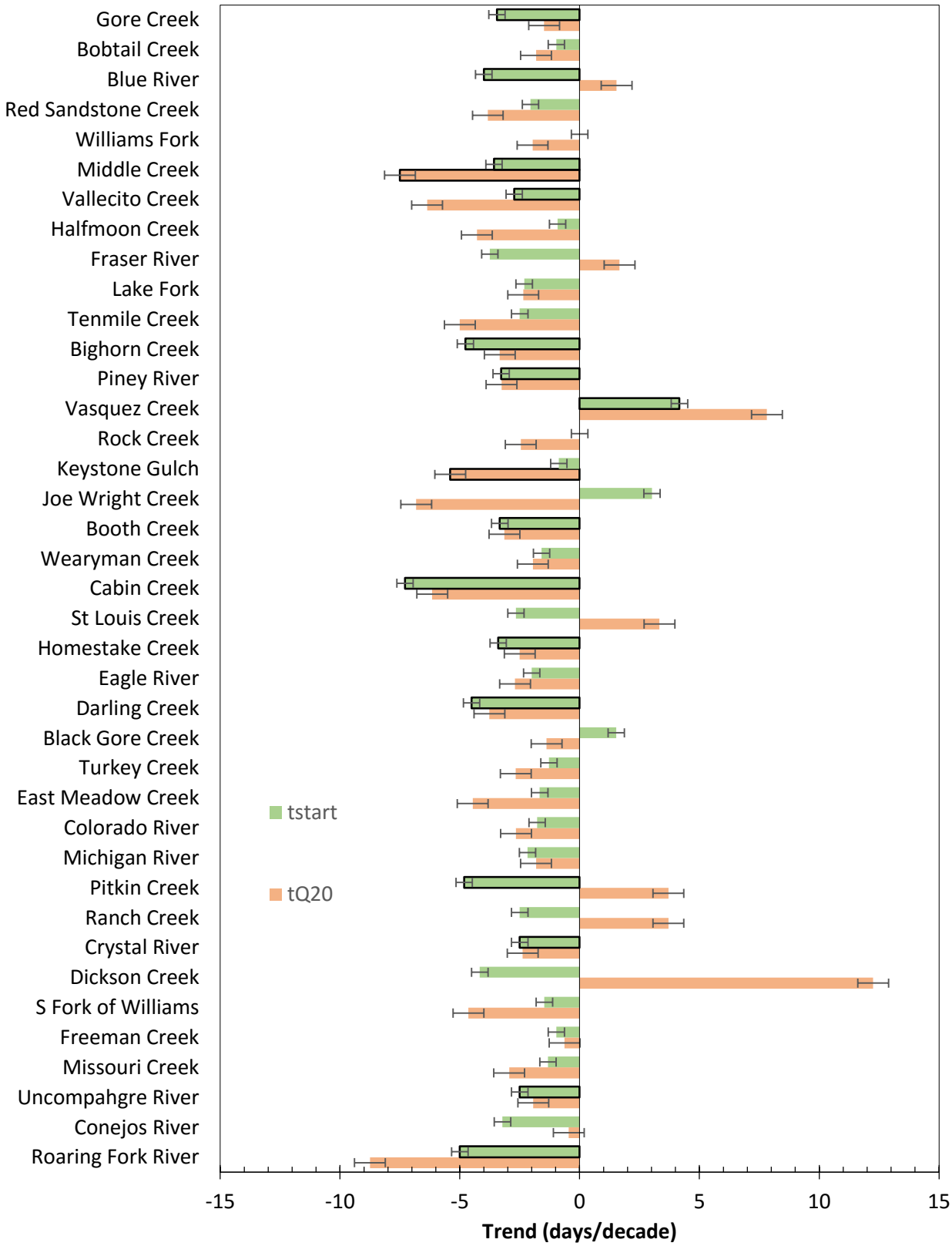

Figure 9. Comparison of trends for t_{start} and t_{Q20}; watersheds are organized by mean elevation. Borders indicate statistical significance ($p < 0.05$).

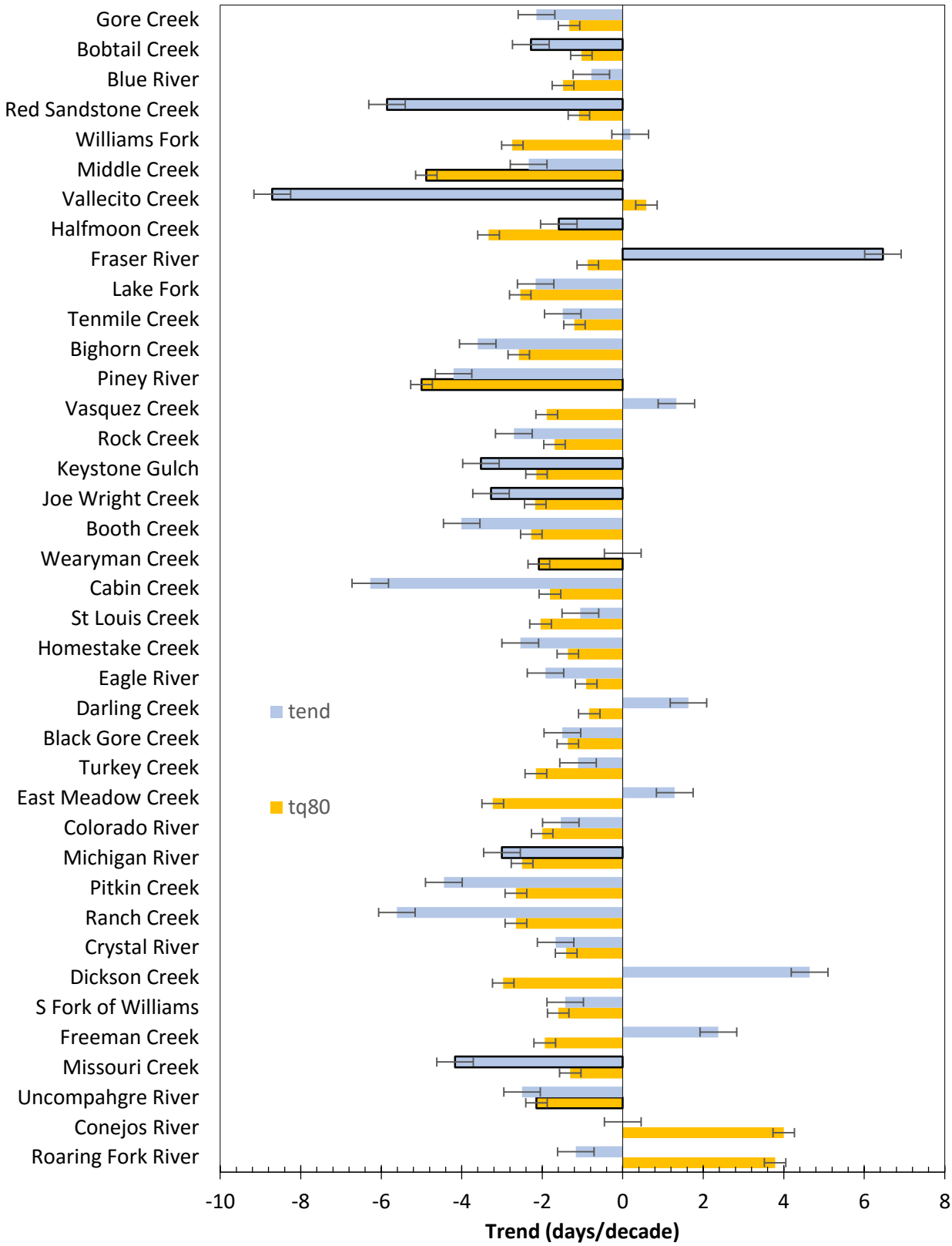

Figure 10. Comparison of trends for t_{end} and t_{Q80}; watersheds are organized by mean elevation. Borders indicate statistical significance ($p < 0.05$).

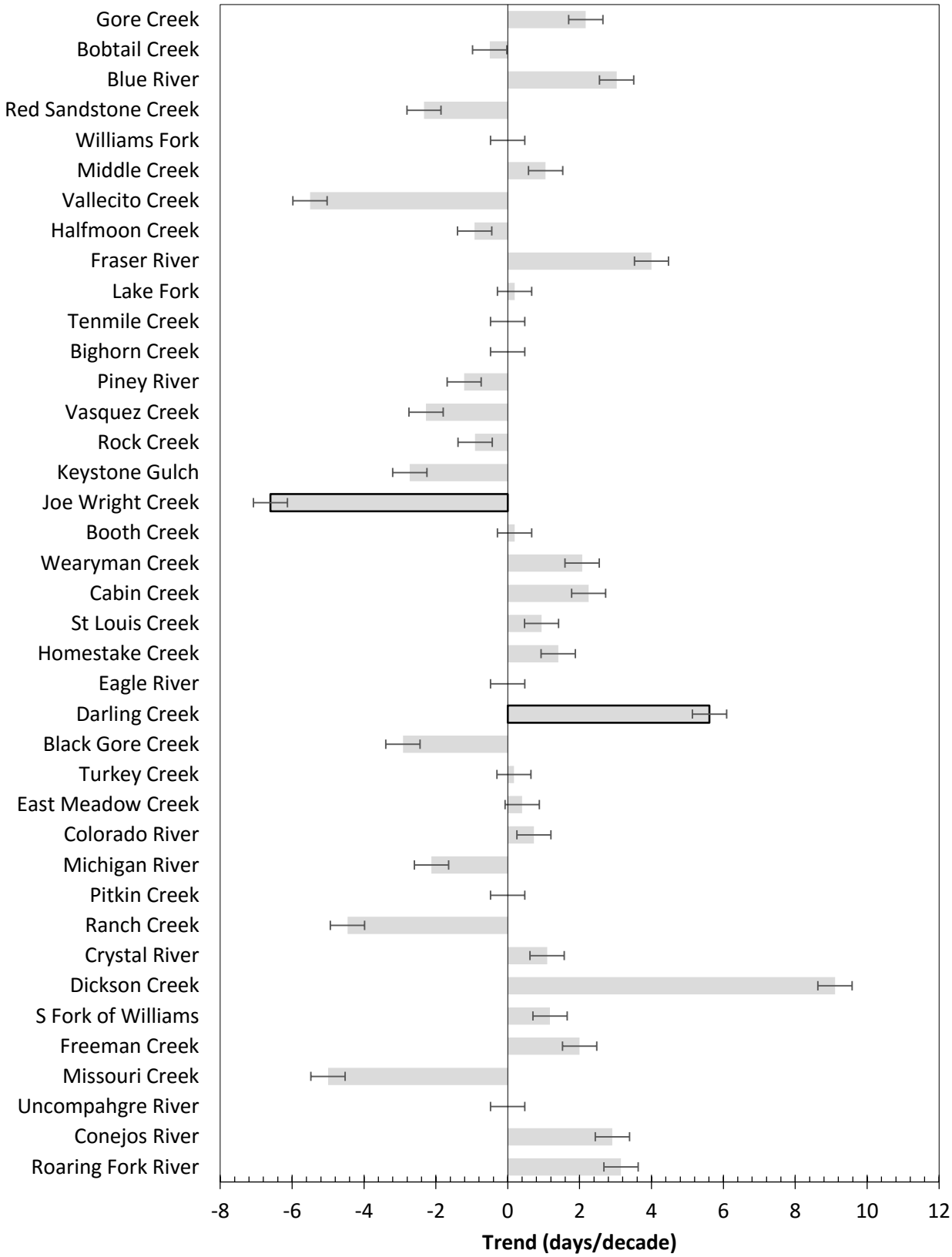

Figure 11. Comparison of trends for $t_{duration}$; watersheds are organized by mean elevation. Borders indicate statistical significance ($p < 0.05$).

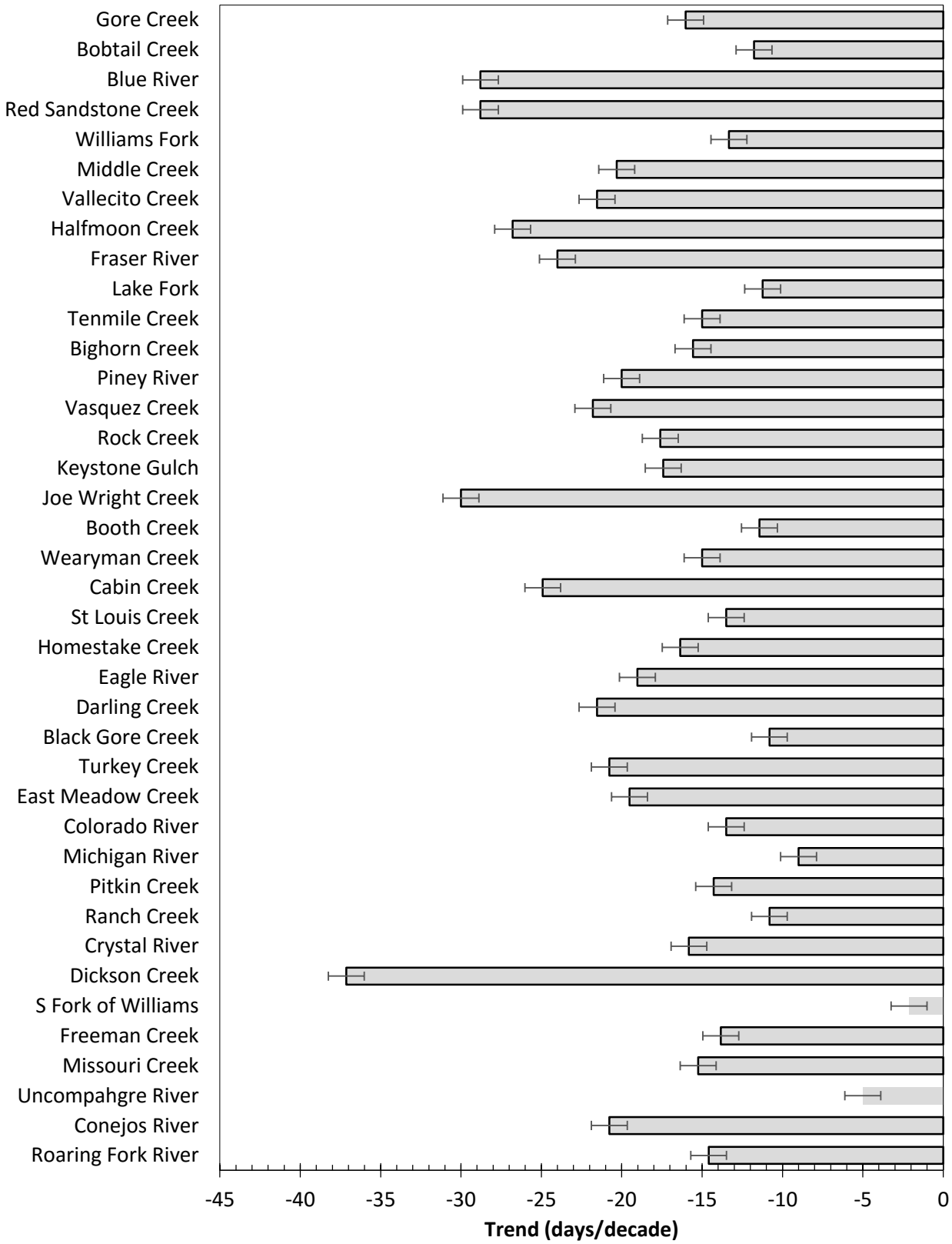

Figure 12. Comparison of trends for $t_{Qduration}$; watersheds are organized by mean elevation. Borders indicate statistical significance ($p < 0.05$).

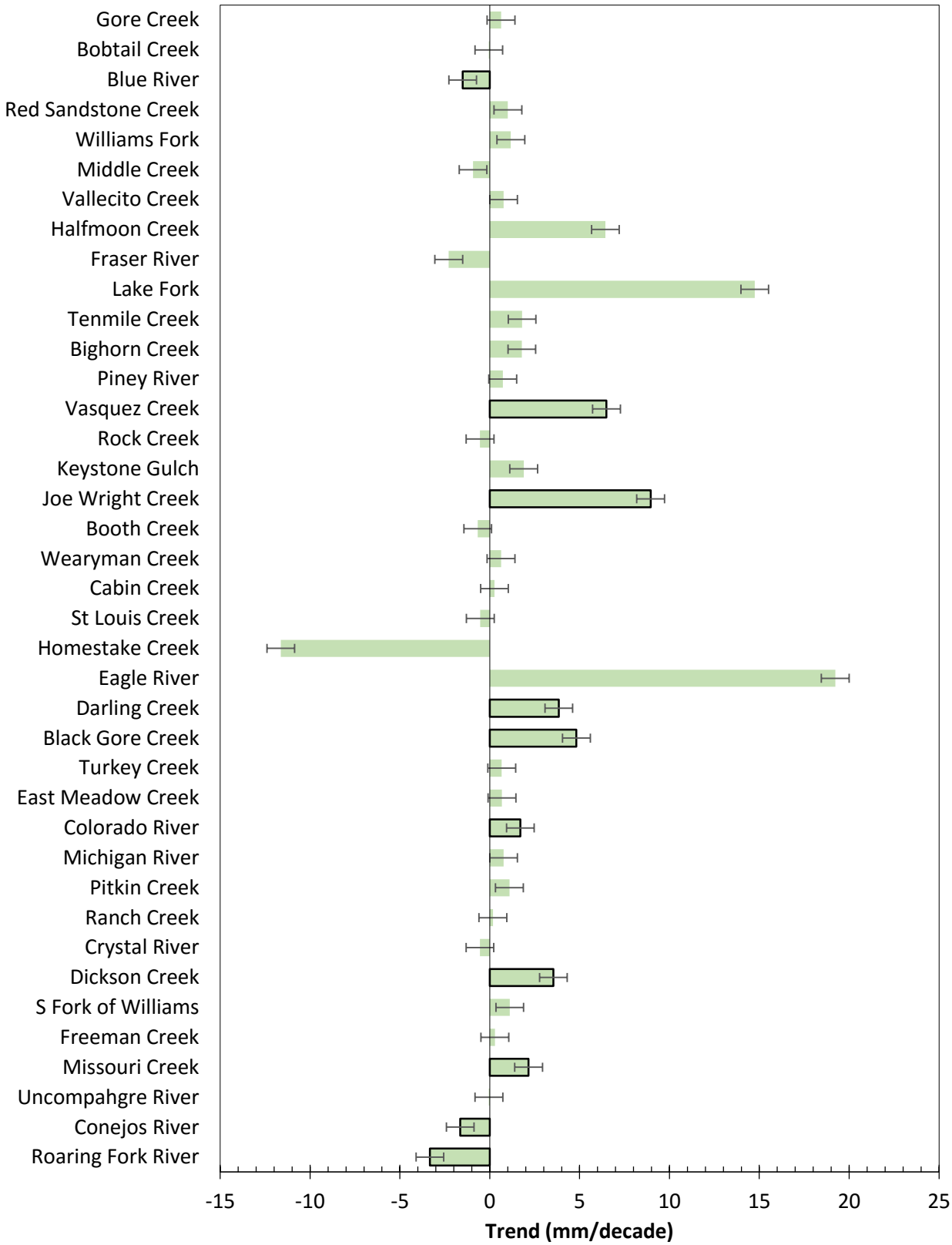

Figure 13. Comparison of trends for Q_{start}; watersheds are organized by mean elevation. Borders indicate statistical significance ($p < 0.05$).

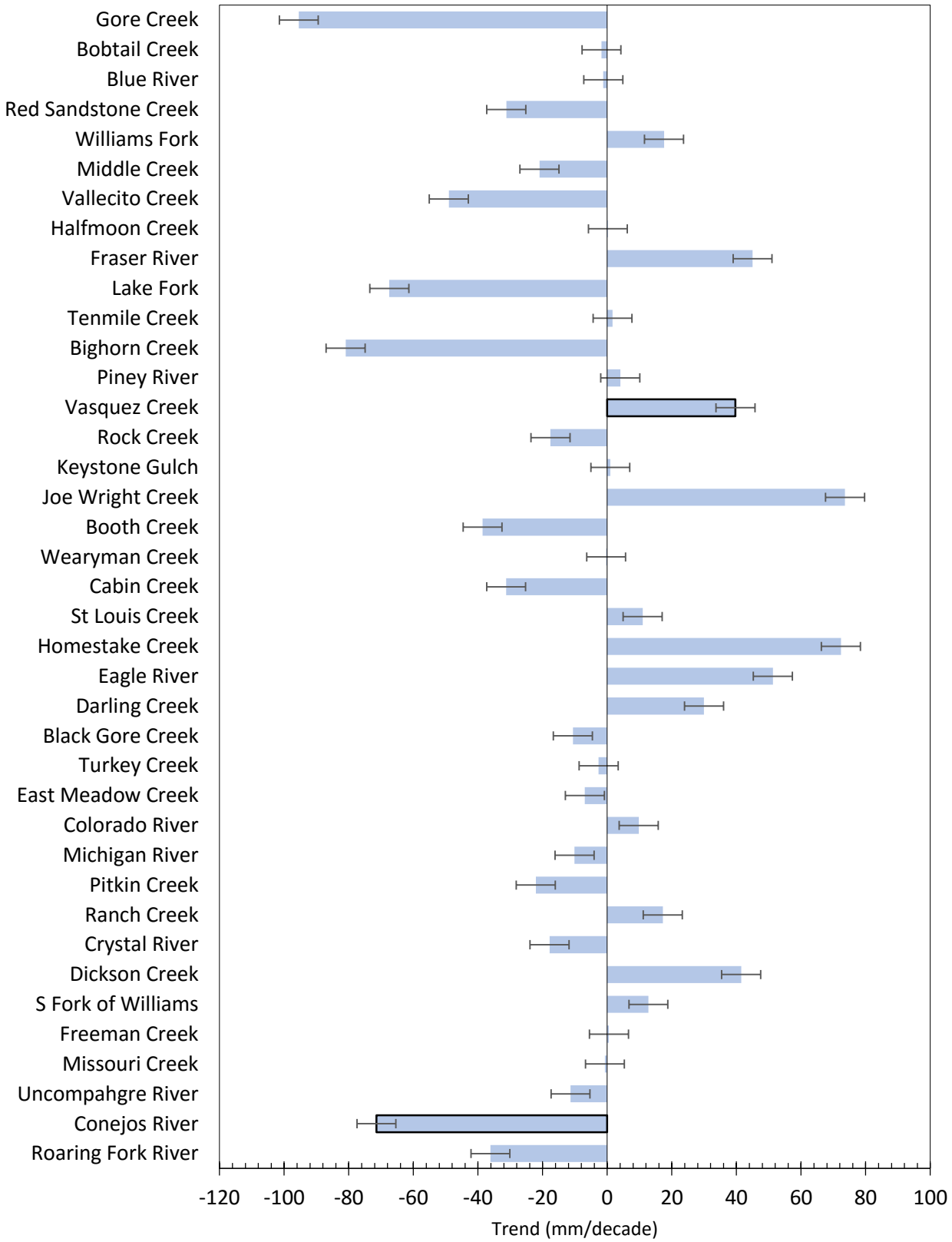

Figure 14. Comparison of trends for Q_{end}; watersheds are organized by mean elevation. Borders indicate statistical significance ($p < 0.05$).

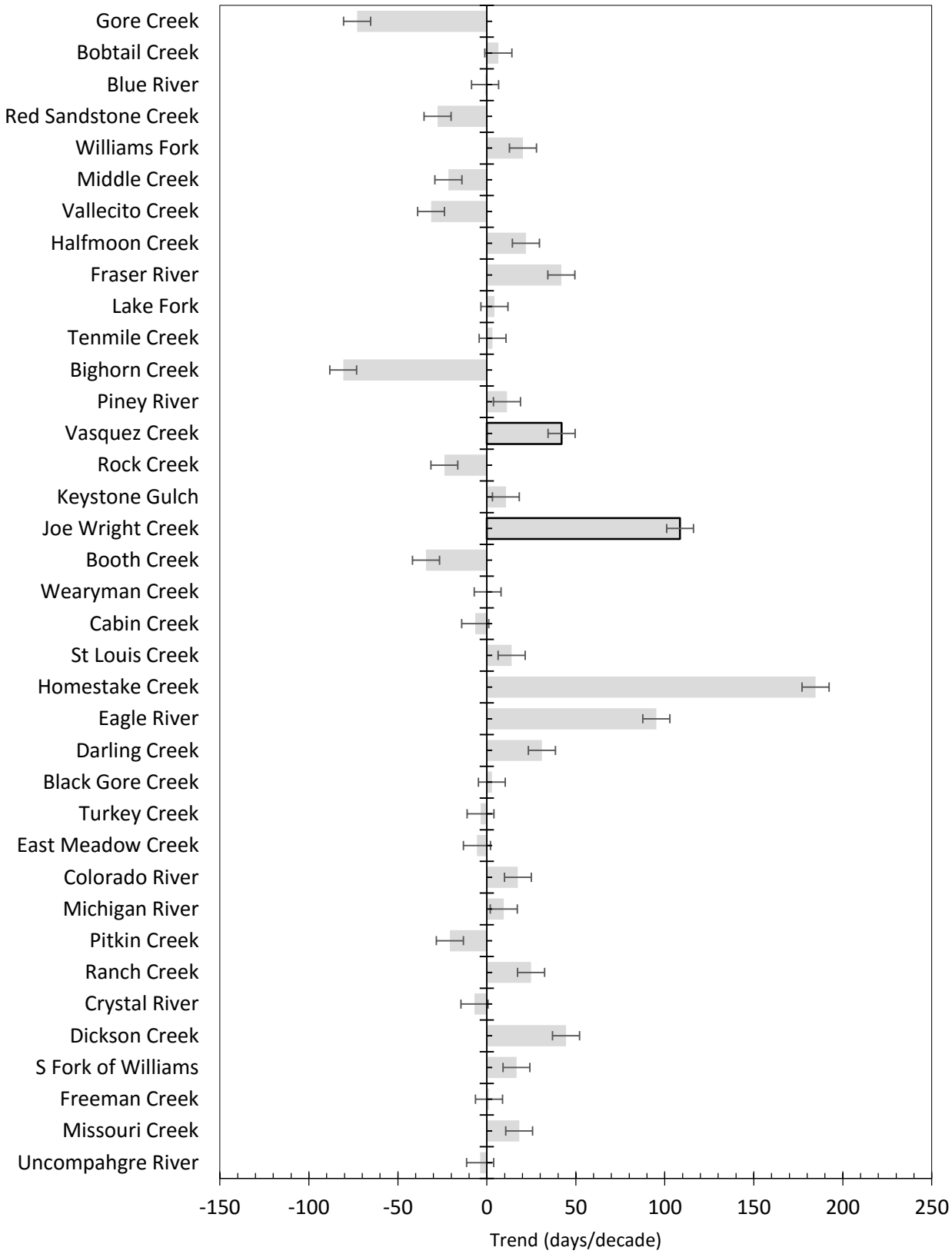

Figure 15. Comparison of trends for Q_{100}; watersheds are organized by mean elevation. Borders indicate statistical significance ($p < 0.05$).

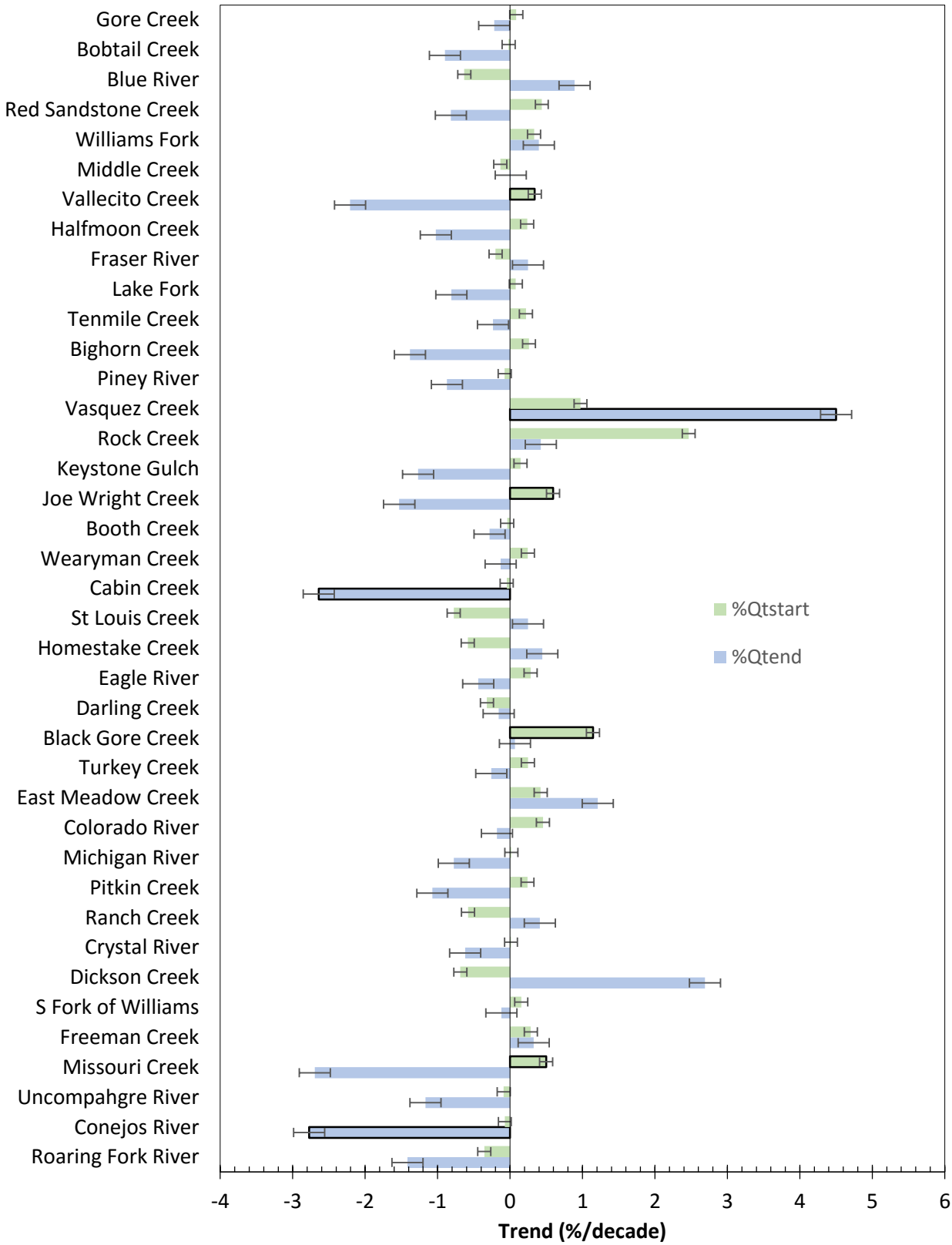

Figure 16. Comparison of trends for $\%Q_{tstart}$ and $\%Q_{tend}$; watersheds are organized by mean elevation. Borders indicate statistical significance ($p < 0.05$).

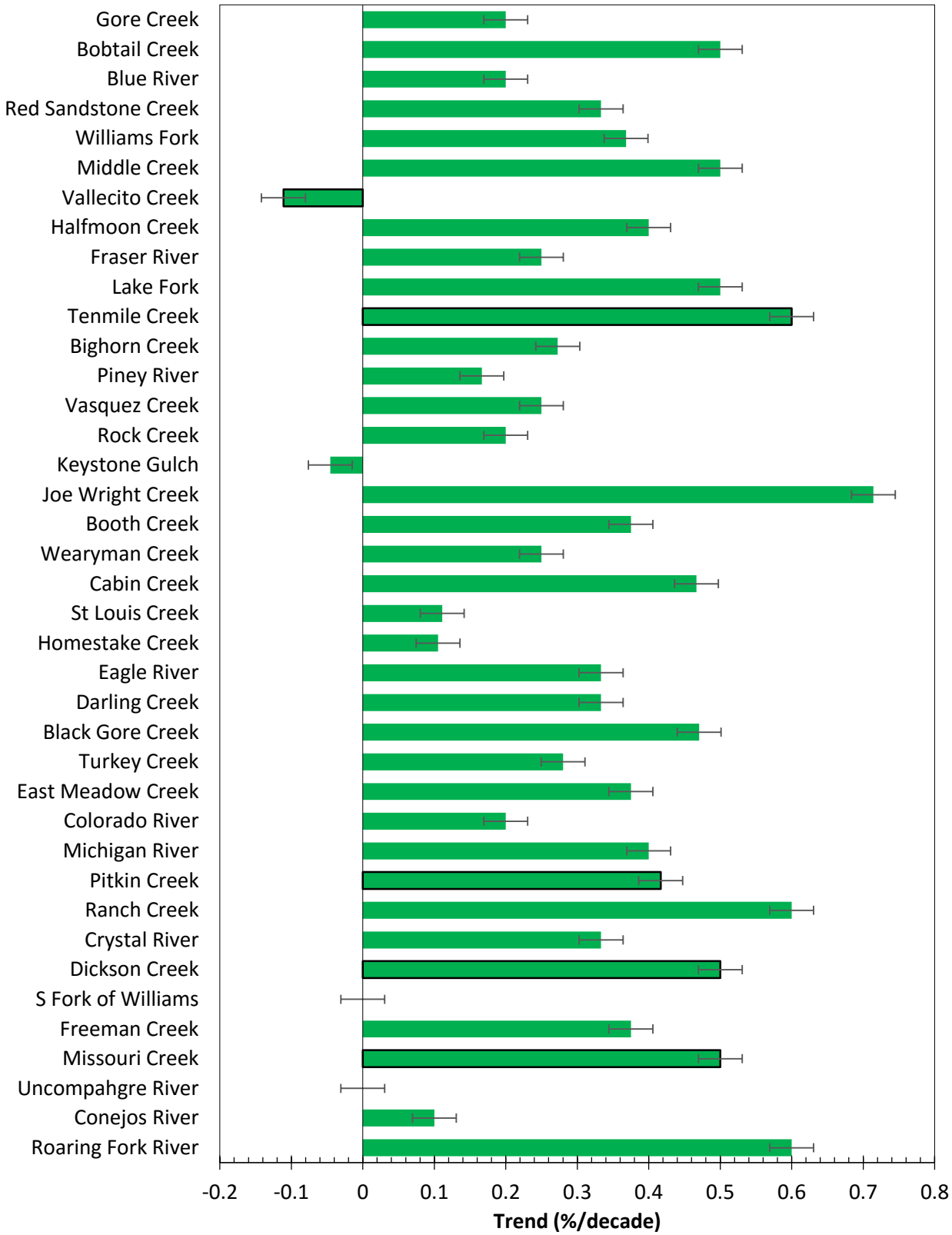

Figure 17. Comparison of trends for NDVI; watersheds are organized by mean elevation. Borders indicate statistical significance ($p < 0.05$).

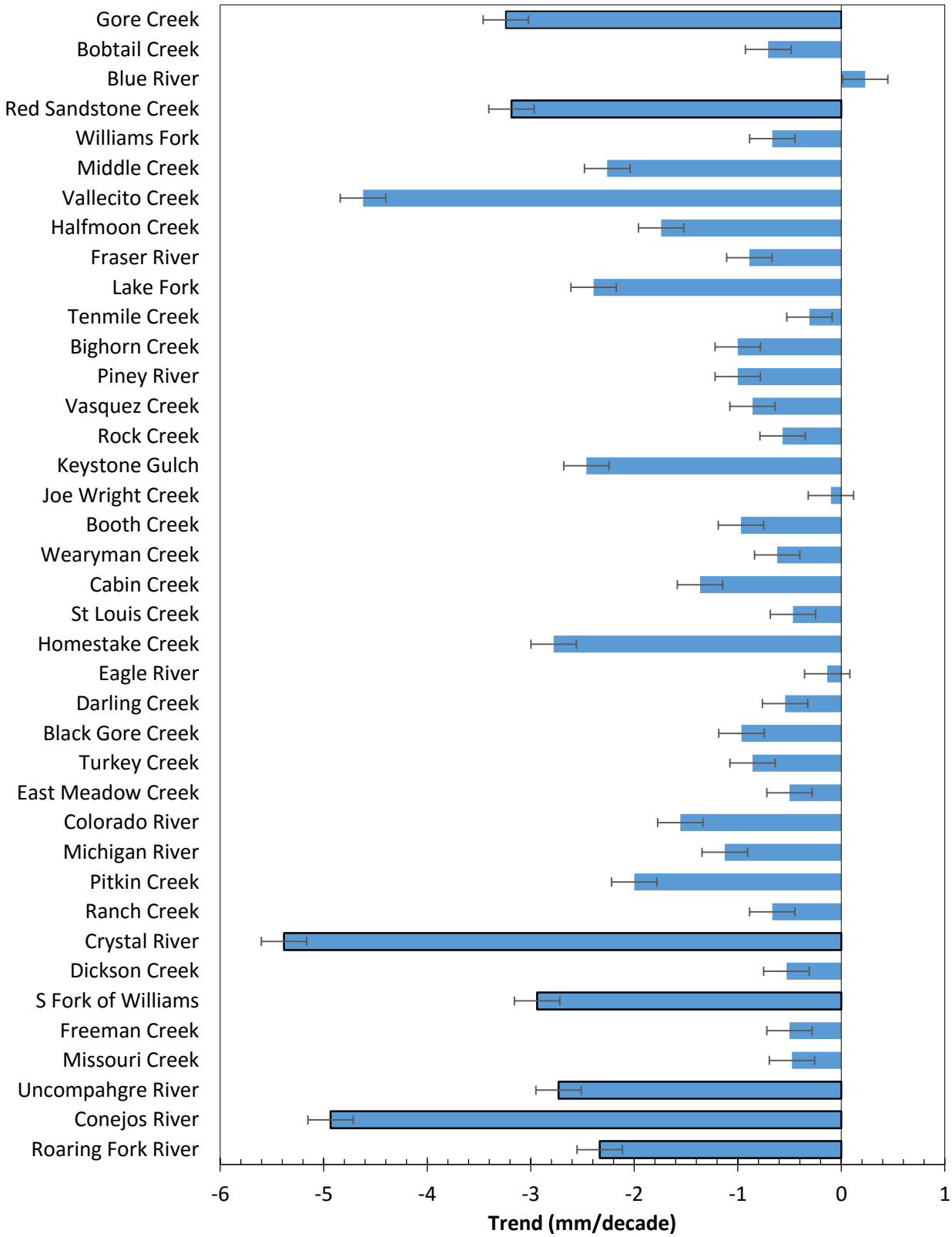

Figure 18. Comparison of trends for winter precipitation; watersheds are organized by mean elevation. Borders indicate statistical significance ($p < 0.05$).

Table 4. Physiographic characteristics of watersheds used in correlation analysis.

Station Name	Solar Radiation (WH/m^2)	Mean Elevation (masl)	Mean Slope (˚)
Bighorn Creek	1647	3369	26
Black Gore Creek	1648	3261	15
Blue River	1607	3546	18
Bobtail Creek	1462	3593	22
Booth Creek	1751	3305	23
Cabin Creek	1628	3287	18
Colorado River	1627	3215	17
Conejos River	1573	2902	9
Crystal River	1498	3097	22
Darling Creek	1569	3266	19
Dickson Creek	1590	3054	13
Eagle River	1637	3270	14
East Meadow Creek	1760	3218	13
Fraser River	1499	3426	19
Freeman Creek	1510	3001	11
Gore Creek	1607	3644	22
Halfmoon Creek	1598	3428	18
Homestake Creek	1548	3271	14
Joe Wright Creek	1629	3313	17
Keystone Gulch	1558	3317	19
Lake Fork	1407	3425	19
Michigan River	1714	3192	17
Middle Creek	1516	3469	22
Missouri Creek	1566	2978	16
Piney River	1707	3369	25
Pitkin Creek	1599	3181	14
Ranch Creek	1629	3166	14
Red Sandstone Creek	1592	3514	21
Roaring Fork River	1491	2494	21
Rock Creek	1672	3323	18
S Fork of Williams	1601	3032	11
St. Louis Creek	1525	3273	17
Tenmile Creek	1604	3424	16
Turkey Creek	1661	3243	17
Uncompahgre River	1444	2938	17
Vallecito Creek	1587	3437	25
Vasquez Creek	1531	3327	16
Wearyman Creek	1539	3297	17
Williams Fork	1624	3486	20

Table 5. Physiographic characteristics of watersheds used in correlation analysis.

* Indicates statistical significance ($p < 0.10$)

** Indicates statistical significance ($p < 0.05$)

	t_{start}	t_{end}	$t_{duration}$	Q_{100}	Q_{start}	Q_{end}	$Q_{duration}$	$\%Q_{tstart}$	$\%Q_{tend}$	t_{Q20}	t_{Q50}	t_{Q80}	$t_{Qduration}$
NDVI	0.05	0.06	-0.05	0.09	0.27*	0.12	0.08	-0.01	0.02	-0.01	0.07	-0.11	-0.16
Winter Precip	0.2	0.3*	0.02	0.28*	0.24	0.48**	0.39**	0.09	0.38**	0.23	0.07	-0.39**	-0.13
Mean Radiation	0.03	-0.22	-0.2	-0.08	0	0	0.08	0.26	0.04	-0.09	-0.25	-0.26	-0.11
Mean Elevation	0.13	-0.14	-0.18	0.01	0.15	-0.04	-0.07	0.12	0.16	-0.01	-0.17	-0.46**	-0.24
Mean Slope	-0.2	-0.38**	-0.17	-0.37**	-0.07	-0.38**	-0.36**	-0.01	-0.23	-0.37**	-0.29*	-0.16	-0.06
Latitude	0.04	0.2	0.1	0.39**	0.11	0.35**	0.23	0.04	0.39**	0.26	0.15	-0.51**	-0.06
Longitude	0.1	-0.3*	0.31*	-0.12	0.05*	-0.11	-0.13**	0.05	-0.14	-0.09	-0.54**	-0.28*	0.07

Chapter 4: Discussion

The COV technique has become a popular streamflow timing metric and has been used in conjunction with the days at which 20% and 80% of flow has passed to examine snowmelt timing in streams. These metrics do not always adequately identify when processes are occurring. In order to address these shortcomings, we developed a new method to better represent snowmelt timing in streamflow and identify any trends related to various timing variables.

Comparison of results from methodologies

Based on NSE and RMSE values of the two methods, the automated estimation is an improvement over using 20% and 80% of flow as proxies for the start and end of snowmelt contribution (Table 2; Table 3; Figure 19; Figure 20). The mean values would be a better predictor than using t_{Q20} or t_{Q80} whereas the automated estimation reasonably predicts t_{start} and t_{end}. The poor performance for tQ20 and tQ80 may be responding to other variables, or, more simply to differences in the total annual discharge volume, and not snowmelt (Whitfield, 2013). While this analysis was only conducted for 3 of the 39 watersheds, the basins chosen were representative of the small, medium, and large watersheds included within this analysis. This method could likely be employed for watersheds with similar characteristics but would need to undergo further verification before being applied to larger basins. Additionally, adjustments should be made to the technique when trying to apply it to watersheds in different climates like the Pacific Northwest, where the transition from a baseflow to snowmelt-dominated watershed is not as easily distinguished.

We then compared the specific dates for the start and end of snowmelt contribution. Using both t_{start} and t_{end} are improvements upon using t_{Q20} and t_{Q80} based on the NSE and RMSE values. These values demonstrate that using the mean of the manually extracted values would have been a better predictor than calculating either t_{Q20} or t_{Q80}, whereas t_{start} and t_{end} are able to predict these days reasonably well.

The calculated trends demonstrate the differences in magnitude as well as statistical significance from the two methods. For the start of snowmelt (Figure 9), in general, the two methods show that snowmelt timing is occurring earlier in the year, but the magnitude for t_{Q20} is larger than what was calculated for t_{start}. For t_{Q20}, there are 6 stations that show snowmelt is occurring later in the year, where t_{start} is happening earlier. We observed greater statistical significance across stations for t_{start}. For the end of snowmelt (Figure 10), trends for both methods show the end of snowmelt contribution is occurring earlier in the year, although trends in t_{end} were larger in magnitude than for t_{Q80}, and we observed greater statistical significance at stations for t_{end}. The larger number of stations with statistically significant trends for the automated methodology also shows that these trends are a reflection of changes taking place within these watersheds.

The two methodologies also result in drastically different trends for the duration of snowmelt contribution (Figure 11; Figure 12). Trends in the automatic estimation ranged from 6.6 days/decade earlier and 9.1 days/decade later with statistical significance at only 2 stations, whereas the COV method had trends that ranged from 2.1 to 37.1 days/decade earlier with statistical significance at 37 stations. Based on the performance of the automatic estimation, the new method is likely better at representing trends that are occurring and the reported trends are more reliable than using the COV method. However,

there are still statistically significant changes that are occurring across a majority of the study sites for the middle 60% flow (t_{Q80}-t_{Q20}), which should not be ignored, especially if there are changes as large as 5 weeks for a given decade (Figure 12). These differences in snowmelt may require changes in operation for reservoirs that currently drawdown in the fall in preparation for spring snowmelt (Ryberg et al., 2016).

Other findings from the COV method show different trends than what were calculated here. Clow (2010) used the Regional Kendall test for trend analysis of his streamflow metrics and found that 43%, 62%, and 36% of stations had trends that were occurring significantly earlier for t_{Q20}, t_{Q50}, and t_{Q80}, respectively; there were no observed trends that were occurring later in the year for any of his metrics. Additionally, Clow (2010) saw trends range in magnitude from 10 days/decade to 8 days/decade for Q20 and Q80, respectively. Using t_{start} and t_{end} produced a range of 11 days/decade and 14 days/decade, respectively. Our calculations using the COV method produced a range of 20 days/decade and 9 days/decade for t_{Q20} and t_{Q80}, respectively. The differences between studies can partially be explained by our use of the Mann-Kendall test, instead of the Regional Kendall test. A recent study demonstrated that using the Regional Kendall test produced trends that were smaller in magnitude than what was observed at individual stations (Fassnacht, 2016). We also used different site selection criteria; specifically this study used a 40-year period, whereas Clow (2010) used a 29-year-record, ending in 2007.

Stewart et al. (2005) examined streamflow trends in the western United States and Canada from 1948 to 2002. They used the COV method in combination with an algorithm that determined the onset of snowmelt contribution (Cayan et al., 2001) that is similar to the method developed here. For Colorado, they observed few statistically significant trends

in the COV, corroborating our findings. However, for the onset, they observed statistical significance at only 1 station out of 15, whereas we found statistical significance at 15 of the 39. Their trends were also larger in magnitude, ranging from 20 days/decade earlier to 20 days/decade later, but the majority of stations were only 5 days/decade earlier, which is similar to our findings. Our shorter length as well as the timing of the study period could explain these differences. Additionally, we used stations that were at higher elevations than Stewart et al. (2005), so perhaps there is greater statistical significance occurring at these higher elevation gauging stations. Using SNOTEL data, Clow (2010) reported that snowmelt is occurring earlier at higher elevations in Colorado.

Besides having a more accurate prediction of the true timing of snowmelt contribution into streamflow, another advantage this new method presents is that we were able to estimate any trends in the total volume of water from snowmelt that passes in a given season. This information will be helpful for water forecasters and managers making decisions about water storage and reservoirs in the future (Gomez-Landesa and Range, 2002).

Trend Correlation

For incoming winter solar radiation, t_{start}, Q_{start}, Q_{end}, $Q_{duration}$, $\%Q_{tstart}$, and $\%Q_{tend}$ had positive correlations whereas t_{end}, $t_{duration}$, Q_{100}, t_{Q20}, t_{Q50}, t_{Q80}, and $t_{Qduration}$ had negative correlations. These were not statistically significant relationships, showing that the solar radiation for each watershed cannot explain the variance in trends. Meromy et al. (2013) used regression trees to determine factors that influence snow accumulation and ablation around SNOTEL sites in Colorado and solar radiation appeared with the greatest frequency, indicating its importance for SWE. In the Sierra Nevadas, solar radiation was identified as

the primary parameter that influenced snowpack accumulation and ablation (Elder et al., 1991), but for the watersheds in this study, solar radiation alone is unable to explain the trends in snowmelt variables.

For NDVI, t_{start}, t_{end}, Q_{100}, Q_{start}, Q_{end}, $Q_{duration}$, $\%Q_{tend}$, and t_{Q50} had positive correlations, whereas $t_{duration}$, $\%Q_{tstar}t$, t_{Q20}, t_{Q80}, and $t_{Qduration}$ had negative correlations, but these were not statistically significant relationships. Changes in land cover and vegetation can influence mountain snowmelt timing by as much as 10 days (Ellis et al., 2013). NDVI had few changes in the watersheds used in this study; however, based on the correlation coefficient, the changes that did occur did not influence the variance on the different snowmelt variables used in this study.

For elevation, t_{start}, Q_{100}, Q_{start}, $\%Q_{tstart}$, and $\%Q_{tend}$ had positive correlations, whereas t_{end}, $t_{duration}$, Q_{end}, $Q_{duration}$, t_{Q20}, t_{Q50}, t_{Q80}, and $t_{Qduration}$ had negative correlations, all these relationships except for t_{Q80} were not statistically significant. Contrary to our study, Jepsen et al. (2016) found that runoff in the Sierra Nevada of California are likely dependent on elevation; a study conducted in western Austria found similar correlation with streamflow and elevation (Kormann et al., 2015). However, the mean elevations of watersheds in this study ranged from 2494 to 3644 masl, whereas the other studies ranged from 1467 to 3137 masl (Kormann et al., 2015; Jepsen et al., 2016), so the relationship between these variables and elevation may be more pronounced with a larger range.

For mean slope, all snowmelt variables had negative relationships (Table 5), and t_{end} (Figure 21), Q_{100}, Q_{end}, $Q_{duration}$, and t_{Q20} had statistically significant relationships ($p < 0.05$); t_{Q50} had a statistically significant relationship with slope ($p < 0.10$). Steeper mean slopes within these watersheds result in earlier timing in the year for t_{end}, t_{Q20}, and t_{Q50} and less

water for Q_{100}, Q_{end}, and $Q_{duration}$. Snowmelt in basins with steep slopes enters streams more quickly than similar basins with shallower slopes (Sueker et al., 2000), which could account for the relationship and subsequent earlier timing for t_{end}, t_{Q20}, and t_{Q50}. Snowpack accumulation is less in steeper watersheds (Elder et al., 1991), causing there to be less total volume during spring snowmelt, which could help account for the relationship of slope and Q_{100}, Q_{end}, and $Q_{duration}$.

Many studies have used climatic indices to attempt to explain the variance in their findings (Stewart et al., 2005; Clow, 2010; Fritze et al., 2011). Precipitation was positively correlated with V_{end}, $V_{duration}$, and $\%Q_{tend}$ ($p < 0.05$) as well as t_{end} and Q_{100} ($p < 0.10$), and negatively correlated with and t_{Q80} ($p < 0.05$); no other variables had a statistically significant correlation with precipitation (Table 5). Changes in precipitation may obscuring any warming that has taken place, which could be why there wasn't correlation with other variables (Stewart et al., 2005). In other systems, social factors like forest disturbance and other ecologic changes have hidden the effects of precipitation on streamflow (Jones et al., 2012), but that is not the case for these watersheds as our NDVI trends indicate few changes across the record. Furthermore, because of the complexity of variables in high elevation, mountain watersheds, we cannot always expect that trends in precipitation will follow observed trends in streamflow (Bard et al., 2015).

Streamflow trends have been well correlated with temperature trends (Stewart et al., 2005; Rauscher et al., 2008; Clow, 2010). However, there are inhomogeneities in the PRISM temperature data at high elevation since these rely on SNOTEL stations that are not consistent over the period of record (Oyler et al., 2015). Thus, we have not included spring temperature in our analysis. Beyond temperature and precipitation, few studies that have

looked at trends in streamflow for snowmelt-dominated watersheds have included correlation of physical characteristics of the watersheds, and several studies do not include any type of correlation (Luce and Holden, 2009; Sagarika et al., 2014).

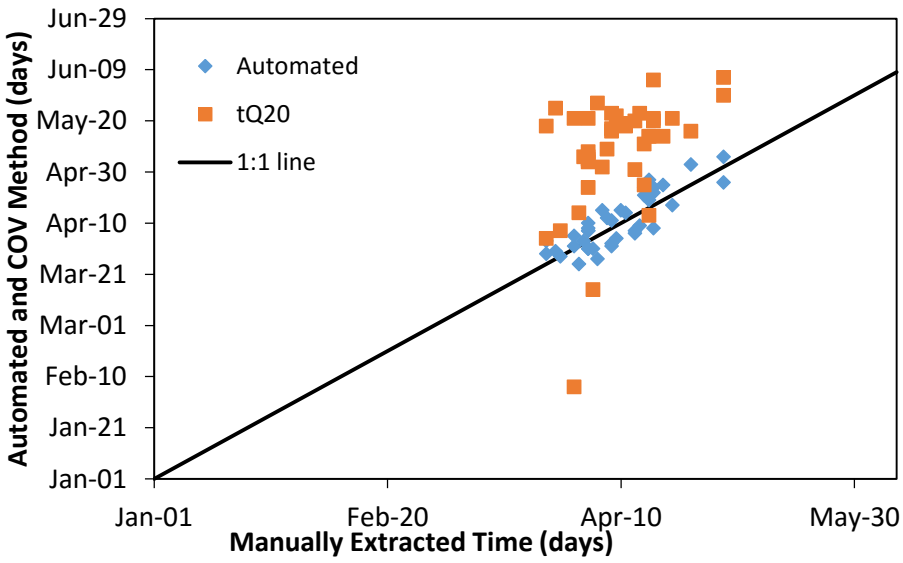

Figure 19. Comparison of the manually extracted start and t_{start} and t_{Q20} from the automated and COV methods.

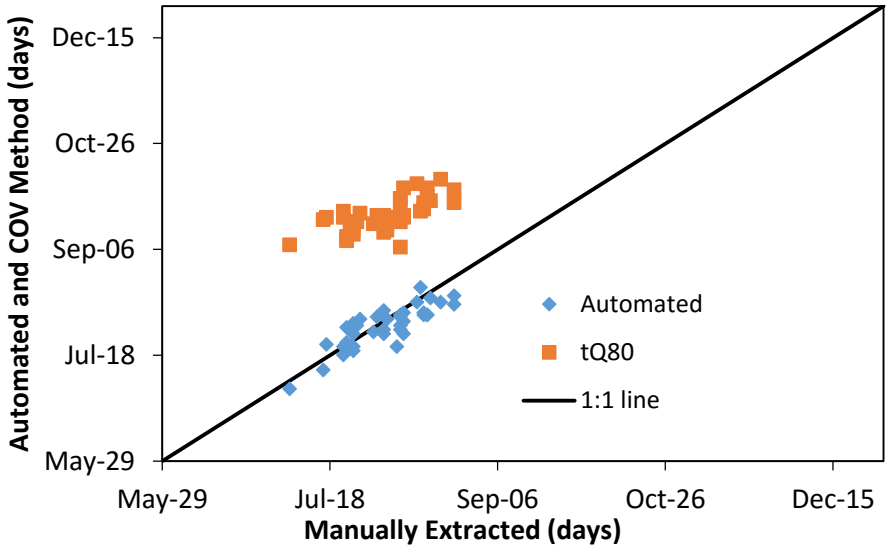

Figure 20. Comparison of the manually extracted start and t_{end} and t_{Q80} from the automated and COV methods.

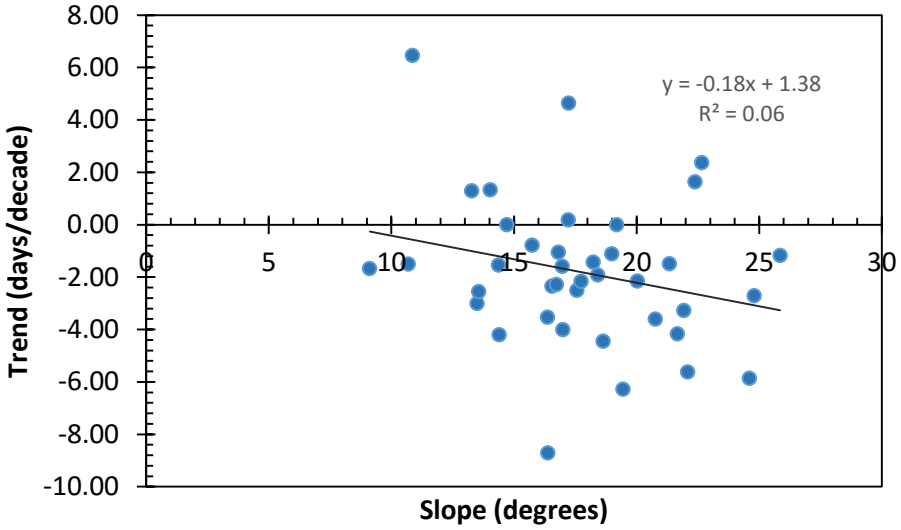

Figure 21. Correlation between slope and trends in t_{end}.

Chapter 5: Conclusions

The goal of this study was to use a new method to estimate start and end of snowmelt contribution to streamflow that used features of the cumulative annual hydrograph from daily discharge data. Using 39 USGS gauging stations, we identified several different variables (t_{start}, t_{end}, $t_{duration}$, Q_{100}, Q_{start}, Q_{end}, $Q_{duration}$, $\%Q_{tstart}$, and $\%Q_{tend}$) related to streamflow over a 40-year period. We also calculated the day at which a given amount of flow had passed, t_{Q20}, t_{Q50}, t_{Q80}, and $t_{Qduration}$, in order to compare the findings of this new methodology against what has commonly been used in the literature. Based on NSE and RMSE values, our new, automated estimation is an improvement over using t_{Q20} and t_{Q80} as predictors for the start and end of snowmelt contribution, respectively.

We also calculated trends in the various snowmelt variables. We observed statistical significance at 15 stations for t_{start} and 9 stations for t_{end}; most trends show earlier timing in the year, by as much as 7 and 8 days/decade for t_{start} and t_{end}, respectively. In order to explain the variance in these calculated trends, we compared the snowmelt variables with different physiographic characteristics (NDVI, winter precipitation, mean radiation, mean slope, mean elevation, latitude, and longitude) of the watersheds; most correlations were not statistically significant. Mean slope was able to explain the variance in trends better than the other characteristics (5 variables where $p < 0.05$ and 1 variables where $p < 0.10$), and had negative correlations with all variables but Pearson's r was only as high as 0.38. Contrary to other studies, precipitation and elevation did not explain the variance in the trends.

Chapter 6: Recommendations

This study used daily streamflow data to develop a method to identify trends in snowmelt contribution based in the Southern Rocky Mountains. Because of the performance of this new model based on NSE and RMSE values compared to using the more common COV method in the literature, we recommend that it be employed more widely when examining trends in snowmelt contribution to streamflow. However, this technique needs to be applied more widely and to different snowmelt-dominated regions to ensure that it performs well under different climatic geographic areas.

We also recommend that future research continue to investigate the potential causes of observed trends. We were unable to consistently explain the variance in the trends in our calculated variables. If the study area is expanded and additional characteristics are included, a multivariate regression should be performed.

Chapter 7: Literature Cited

Bales, R. C., N. P. Molotch, T. H. Painter, M. D. Dettinger, R. Rice, and J. Dozier (2006), Mountain hydrology of the western United States, *Water Resources Research*, *42*, W08432, doi:10.1029/2005WR004387.

Bard, A, B Renard, M Lang, I Giuntoli, J Korck, G Koboltschnig, M Janza, M d'Amico, and D Volken (2015), Trends in the hydrologic regime of Alpine rivers, *Journal of Hydrology*, *529*, 1823-1837.

Barnett, T. P., J. C. Adams, and D. P. Lettenmaier (2005), Potential impacts of a warming climate on water availability in snow-dominated regions, *Nature*, *438*, 303-309.

Cayan, DR, SA Kammerdiener, MD Dettinger, JM Caprio, and DH Peterson (2001), Changes in the onset of spring in the western United States, *Bulletin of the American Meteorological Society*, *82*, 399-415.

Clow, D. W. (2010), Changes in timing of snowmelt and streamflow in Colorado: A response to recent warming, *Journal of Climate, 23,* 2293-2306.

Court, A. (1962), Measures of Streamflow Timing, *Journal of Geophysical Research*, *67(11),* 4335-4339.

Elder, K, J Dozier, and J Michaelsen (1991), Snow accumulation and distribution in an alpine watershed, *Water Resources Research*, *27*, 1541-1552.

Ellis, CR, JW Pomery, and TE Link (2013), Modeling increases in snowmelt yield and desynchronization resulting from forest gap-thinning treatments in a northern mountain headwater basin, *Water Resources Research*, *49*, 936-949, doi:10.1002/wrcr.20089.

Fassnacht, SR (2006), Upper versus lower Colorado River sub-basin streamflow: characteristics, runoff estimation, and model simulation, *Hydrological Processes*, *20*, 2187-2205, doi:10.1002/hyp.6202.

Fassnacht, SR., ML Cherry, NBH Venable, and F Saavedra (2016), Snow and albedo climate change impacts across the United States Northern Great Plains, *The Cryosphere*, *10*, 329-339, doi:10.5194/tc-10-329-2016.

Fritze, H, IT Stewart, and E Pebesma (2011), Shifts in western North American Snowmelt Runoff Regimes for the Recent Warm Decades, *Journal of Hydrometeorology*, *12*, 989-1006, doi: 10.1175/2011JHM1360.1.

Gomez-Landesa, E and A Range (2002), Operational snowmelt runoff forecasting in the Spanish Pyrenees using the snowmelt runoff model, *Hydrological Processes*, *16*, 1583-1591, doi:10.1002/hyp.1022.

Harpold, A., P. Brooks, S. Rajagopal, I. Heidbuchel, A. Jardine, and C. Stielstra (2012), Changes in snowpack accumulation and ablation in the intermountain west, *Water Resources Research*, *48*, W11501, doi:10.1029/2012WR011949.

Jepsen, SM, TC Harmon, MW Measows, and CT Hunsaker (2016), Hydrogeologic influence on changes in snowmelt runoff with climate warming: Numerical experiments on a mid-elevation catchment in the Sierra Nevada, USA, *Journal of Hydrology*, *533*, 332-342.

Jones, JA, IF Creed, KL Hatcher, RJ Warren, MB Adams, MH Benson, E Boose, WA Brown, JL Campbell, A Covich, DW Clow, CN Dahm, K Elder, CR Ford, NB Grimm, DL Henshaw, KL Larson, ES Miles, KM Miles, SD Sebestyen, AT Spargo, AB Stone, JM Vose, and MW Williams (2012), Ecosystem Processes and human influences regulate streamflow response to climate change at long-term ecological research sites, *BioScience*, *62(4)*, 390-404.

Johnson, F. A. (1964), Comments on paper by Arnold Court, 'Measures of streamflow timing', *Journal of Geophysical Research*, *69*, 3525-3527.

Kormann, C, T Francke, M Renner, and A Bronstert (2015), Attribution of high resolution streamflow trends in Western Austria—an approach based on climate and discharge station data, *Hydrology and Earth System Sciences*, *19*, 1225-1245, doi:10.5194/hess-19-1225-2015.

Leung, LR, Y Qian, X. Bian, WM Washington, J Han, and JO Roads (2004), Mid-century ensemble regional climate change scenarios for the western United States, *Climatic Change*, *62*, 75-113.

Luce, CH and ZA Holden (2009), Declining annual streamflow distributions in the Pacific Northwest United States, 1948-2006, *Geophysical Research Letters*, *36*, L16401, doi:10.1029/2009GL039407.

Meromy, L, NP Molotch, TE Link, SR Fassnacht, and R Rice (2013), Subgrid variability of snow water equivalent at operational snow stations in the western USA, *Hydrological Processes*, *27*, 2382-2400, doi:10.1002/hyp.9355.

Moore, J, JT Harper, and MC Greenwood (2007), Significance of trends toward earlier snowmelt runoff, Columbia and Missouri Basin headwaters, western United States, *Geophyical Research Letters*, *34*, L16402, doi:10.1029/2007GL031022.

Oyler, J. W., S. Z. Dobrowski, A. P. Ballantyne, A. E. Klene, and S. W. Running (2015), Artificial amplification of warming trends across the mountains of the western United States, *Geophysical Research Letters*, doi:10.1002/2014GL062803.

Rauscher, S. A., J. S. Pal, N. S. Diffenbaugh, and M. M. Benedetti (2008), Future changes in snowmelt-driven runoff timing over the western US, *Geophysical Research Letters*, *35*, doi:10.1029/2008FL034424.

Ryberg, KR, FA Akyuz, GJ Wiche, and W Lin (2016), Changes in seasonality and timing of peak streamflow in snow and semi-arid climate of the north-central United States, 1910-2012, *Hydrological Processes*, *30*, 1208-1218, doi:10.1002/hyp.10693.

Sagarika, S, A Kalra, and S Ahmad (2014), Evaluating the effect of persistence on long-term trends and analyzing step changes in streamflows of the continental United States, *Journal of Hydrology*, *517*, 36-53.

Salmi, T, A Maatta, P Anttila, TR Airola, and T Amnell (2002), Detecting trends of annual values of atmospheric pollutants by the Mann-Kendall Test and Sen's Slope Estimates: The Excel Template Application Makesens, Publication on Air Quality, Finnish Meteorological Institute, Helsinki.

Satterlund, D. R. and A. R. Eschner (1965), Land use, snow, and streamflow regimen in central New York, *Water Resources Research*, *1(3)*, 397-405.

Schlaepfer, DR, WK Lauenforth, and JB Bradford (2012), Consequences of declining snow accumulation for water balance of mid-latitude dry regions, *Global Change Biology*, *18*, 1988-1997.

Serreze, MC, MP Clark, and RL Armstrong (1999), Characteristics of the western United States snowpack from snowpack telemetry (SNOTEL) data, *Water Resources Research*, *35(7)*, 2145-2160.

Seuker, JK, JN Ryan, C Kendall, and RD Jarrett (2000), Determination of hydrologic pathways during snowmelt for alpine/subalpine basins, Rocky Mountain National Park, Colorado, *Water Resources Research*, *36*, 63-75.

Stewart, IT, DR Cayan, and MD Dettinger (2004), Changes in snowmelt runoff timing in western North America under a 'Business as Usual' climate change scenario, *Climatic Change*, *62*, 217-232.

Stewart, IT, DR Cayan, and MD Dettinger (2005), Changes toward earlier streamflow timing across Western North America, *Journal of Climate*, *18*, 1136-1155.

Stewart, IT (2009), Changes in snowpack and snowmelt runoff for key mountain regions, *Hydrological Processes*, *23*, 78-94.

Wehner, C (2016), Effect of Mountain Pine Beetle on streamflow generation mechanisms, Unpublished M.S. Thesis, Watershed Science, Colorado State University, Fort Collins, CO, USA, 75pp.

Westerling, A. L., H.G. Hidalgo, D.R. Cayan, and T.W. Swetnam (2006), Warming and earlier spring increase western U.S. forest wildfire activity, *Science*, *313*, 940-943.

Whitfield, P. H. (2013), Is 'Centre of Volume' a robust indicator of changes in snowmelt timing?, *Hydrological Processes*, *27*, 2691-2698.

Yue, S, P Pilon, B Phinney, and G Cavadias (2002), The influence of autocorrelation on the ability to detect trend in hydrological series, *Hydrological Processes*, *16*, 1807-1829.

Yue, S and P Pilon (2005), Probability distribution type of Canadian annual minimum streamflow, *Hydrological Sciences Journal*, *50*, 427-438.

Chapter 8: List of Abbreviations

Q_{100}	Total flow for a given
t_{start}	Start of snowmelt contribution to streamflow (introduced methodology)
t_{end}	End of snowmelt contribution to streamflow (introduced methodology)
$t_{duration}$	Duration of snowmelt contribution (introduced methodology)
$\%Q_{tstart}$	Percentage of total annual flow that has passed at t_{start}
$\%Q_{tend}$	Percentage of total annual flow that has passed at t_{end}
Q_{start}	Volume of water that has passed at t_{start}
Q_{end}	Volume of water that has passed at t_{end}
$Q_{duration}$	Total volume of water that passed between t_{start} and t_{end}
t_{Q20}	Day at which 20% of the total annual flow has passed, previously been used as a proxy for the start of snowmelt contribution
t_{Q50}	Day at which 50% of the total annual flow has passed, referred to as Center of Volume (COV) or Center Timing (CT) in the literature
t_{Q80}	Day at which 80% of the total annual flow has passed, previously been used as a proxy for the end of snowmelt contribution
$t_{Qduration}$	Duration of snowmelt contribution calculated from subtracting t_{Q20} from t_{Q80}